Evolution of limb development in cephalopod mollusks

Oscar A. Tarazona[1,2], Davys H. Lopez[1], Leslie A. Slota[2], and Martin J. Cohn[1,2,#]

[1]Department of Molecular Genetics and Microbiology, [2]Department of Biology, UF Genetics Institute, University of Florida, Gainesville, FL 32610 USA.

[#]Corresponding author: mjcohn@ufl.edu

Abstract

Cephalopod mollusks evolved numerous anatomical innovations, including specialized arms and tentacles, but little is known about the developmental mechanisms underlying the evolution of cephalopod limbs. Here we show that all three axes of cuttlefish limbs are patterned by the same signaling networks that act in vertebrates and arthropods, although they evolved limbs independently. In cuttlefish limb buds, *Hedgehog* is expressed anteriorly. Posterior transplantation of *Hedgehog*-expressing cells induced mirror-image limb duplications. Bmp and Wnt signaling, which establishes dorsoventral polarity in vertebrate and arthropod limbs, is similarly polarized in cuttlefish. Inhibition of the dorsal Bmp signal caused ectopic expression of *Notum,* a ventral sucker field marker, and development of ectopic suckers. Cuttlefish limbs also show proximodistally regionalized expression of *Htx*, *Exd, Dll*, *Dac*, *Sp8/9*, and *Wnt* genes*,* which delineate arm and tentacle sucker fields. These results suggest that cephalopod limbs evolved by parallel activation of an ancient genetic program for appendage development that was present in the bilaterian common ancestor.

Introduction

Animal appendages have widely varying morphologies and perform a multitude of functions, including locomotion, feeding, and reproduction (Nielsen, 2012; Ruppert et al., 2004). Limbs evolved independently on multiple occasions, and many animal lineages show no evidence of shared ontogenetic or morphological precursors of appendages (Minelli, 2003; Pueyo & Couso, 2005; Shubin et al., 1997). This has led to the view that appendages in different clades of Bilateria are non-homologous morphological innovations that arose by convergent evolution (Nielsen, 2012; Ruppert et al., 2004). However, despite more than 500 million years of divergence, the independently evolved limbs of arthropods and vertebrates share developmental genetic similarities (Pueyo & Couso, 2005; Shubin et al., 1997; Tabin et al., 1999).

These discoveries led to debate over whether the genetic program for appendage development evolved in the common ancestor of all bilaterians in the early Cambrian (>500 millions of years ago), or whether arthropod and vertebrate appendages have undergone rampant convergence of developmental programs (Minelli, 2000, 2003; Panganiban et al., 1997; Pueyo & Couso, 2005; Shubin et al., 1997; Tabin et al., 1999). A major obstacle to resolving this question is that the evidence of a conserved program derives almost exclusively from Ecdysozoa and Deuterostomia (Pueyo & Couso, 2005; Shubin et al., 1997), and little is known about molecular mechanisms of limb development in Spiralia, the third major superphylum of Bilateria (Prpic, 2008; Winchell & Jacobs, 2013; Winchell et al., 2010).

Within spiralians, the phylum Mollusca is the largest lineage, displaying a rich diversity of body plans (*Figure 1A*) dating back to the Cambrian explosion (Ruppert et al., 2004; Smith et al., 2011). The evolution of arms and tentacles in cephalopod mollusks contributed to the successful adaptive radiation of these agile marine predators (Kroger et al., 2011; Ruppert et al., 2004). Cephalopod limbs are highly muscular appendages that bear cup-shaped suckers on their ventral sides. Arms are short and have suckers along the entire ventral surface (*Figure 1B and C*), whereas tentacles are longer, retractable appendages with suckers restricted to a distal pad (*Figure 1D and E*). Tentacles are thought to be specialized serial homologs of the arms (Arnold, 1965; Lemaire, 1970; Shigeno et al., 2008) and are present in decapods (squid and cuttlefish) but absent in nautilids and octopods. Limbs likely evolved *de novo* in cephalopods (*Figure 1A*), since no homologous precursor structures have been identified in any other mollusk lineages (Lee et al., 2003; Shigeno et al., 2008). To test the hypothesis that cephalopod limbs evolved by recruitment of an ancient gene regulatory network for appendage development that is conserved across Bilateria, we investigated arm and tentacle development in embryos of the cuttlefish, *Sepia officinalis*.

Results

Development of arms and tentacles in the cuttlefish (*Sepia officinalis*)

Cuttlefishes are decapod cephalopods that bear eight arms and two tentacles (*Figure 1B-E; Figure 1- supplementary movies 1 and 2*). Fertilized cuttlefish eggs display superficial cleavage, and scanning electron microscopy and optical projection tomography show that most embryonic development is restricted to the animal pole (*Figure 1H and I*). The first sign of limb formation is observed at stage 16, when all ten limb primordia (5 on each side) can be detected as small swellings around the periphery of a flat-shaped embryo, which lies at the top of the large yolk mass (*Figure 1H and M*). Analysis of the mitotic marker phospho-histone H3 (PHH3) at stage 15 revealed localized clusters of PHH3-positive cells in each of the early limb primordia (*Figure 1F and G*), indicating that initiation of limb outgrowth is caused by localized cell proliferation. Discrete limb buds are observed from stage 17 (*Figure 1I and N; Figure 1- supplementary movie 3*). As the embryo begins to rise-up on the animal pole around stage 19, the limb buds start to elongate along the proximodistal axis (*Figure 1J and O; Figure 1- supplementary movie 4*), and by stage 24, the differential length and morphology of arms relative to tentacles is apparent (*Figure 1L; Figure 1- supplementary movie 5)*.

Analysis of sucker development showed that a sucker field primordium initially forms as a narrow proximodistal ridge along the ventral surface of each limb (evident by stage 21; *Figure 1P*). At later stages, the sucker field ridge cleaves superficially, segregating

sucker buds from proximal to distal (*Figure 1Q*). As the arms elongate, the sucker buds are laid down on the entire ventral surface of each arm (*Figure 1L and R*; *Figure 1- figure supplement 1A and C-G*), forming four parallel rows across the anteroposterior axis (*Figure 1C; Figure 1- figure supplement 1A*). In the tentacles, the primordial sucker band is restricted to the distal tip, where sucker buds form in eight rows along the anteroposterior axis of the tentacle sucker pads (*Figure 1D; Figure 1- figure supplement 1B*). The full complement of immature sucker bud rows is present on each limb at hatching, and differentiation of the suckers continues during post-hatch development (*Figure 1- figure supplement 1H and I*).

Molecular analysis of cuttlefish limbs reveals conservation of proximodistal, anteroposterior, and dorsoventral patterning networks

To test the hypothesis that cuttlefish limb development is regulated by the same molecular mechanisms that pattern arthropod and vertebrate limbs, despite their independent evolutionary origins, we cloned and characterized cuttlefish orthologs of genes that pattern all three limb axes , and then analyzed their expression patterns during cuttlefish limb development (*Figure 2* and *Figure 2- figure supplements 1-10*).

Partial sequences of cuttlefish cDNAs were isolated by rt-PCR and preliminary identities were determined by comparison with NCBI sequence databases, including the octopus genome. Molecular phylogenetic reconstructions were then made by maximum likelihood phylogenetic inference using the best amino acid substitution model for each gene family (see Materials and Methods for details). Tree topologies with well-supported

bootstrap values showed the position of each cuttlefish gene within the targeted gene families, which included *Wnt*, *Tcf/Lef*, *Frizzled* (*Fzd*), *Dachsund* (*Dac/Dach*), *Notum*, *Patched* (*Ptc/Ptch*), *Hedgehog* (*Hh*), *Bone morphogenetic protein* (*Bmp*), *Specificity protein* (*Sp*), and the ANTP and TALE homeobox gene families (trees are shown in *Figure 2- figure supplements 1-10* and are described below; the data set used in the phylogenetic analyses is provided in *Figure 2 - Supplementary file 1*).

Within the Wnt family of cell signaling proteins, we isolated cuttlefish orthologs of *Wnt1*, *Wnt2*, *Wnt5,* and *Wnt7* (*Figure 2-figure supplement 1*). Phylogenetic analysis of cuttlefish transcription factors identified *Tcf3/4*, an ortholog of arthropod *Pangolin* and a pro-ortholog of vertebrate *Tcf3* and *Tcf4* (*Figure 2-figure supplement 2*), *Dac*, a pro-ortholog of vertebrate *Dach1* and *Dach2* (*Figure 2-figure supplement 3*), and *Sp8/9*, a pro-ortholog of vertebrate *Sp8* and *Sp9* (*Figure 2-figure supplement 4*). We also identified numerous homeobox genes, which phylogenetic analyses confirmed to be *Dll*, a pro-ortholog of vertebrate *Dlx* genes, *Exd*, a pro-ortholog of vertebrate *Pbx* genes, *Htx*, a pro-ortholog of vertebrate *Meis1* and *Meis2*, and *Engrailed,* a pro-ortholog of vertebrate *En1* and *En2* (*Figure 2-figure supplement 5*).

In addition, we cloned the Wnt extracellular inhibitors *Notum* and *Sfrp-1/2/5*, and the Wnt co-receptor *Fzd9/10* (*Figure 2-figure supplements 6 and 7*). Cuttlefish possess a *Bmp-2/4* gene that is an ortholog of arthropod *Dpp* and a pro-ortholog of vertebrate *Bmp2* and *Bmp4* (*Figure 2-figure supplement 8*), a *Hh* gene (Grimaldi et al., 2008) that we show to be a pro-ortholog of the vertebrate hedgehog family (*Figure 2-figure*

supplement 9), and a gene encoding the Hh receptor *Patched*, a pro-ortholog of vertebrate *Ptch1* and *Ptch2* (*Figure 2-figure supplement 10*). The cuttlefish *Sfrp* ortholog that we identified as *Sfrp1/2/5* was annotated incorrectly in the octopus genome as *Frizzled1* (*Figure 2-Supplementary file 1*). We also found two *Sp8/9* genes in the octopus genome (*Figure 2-Supplementary file 1*), and the cuttlefish *Sp8/9* gene shows clear orthology to only one of the two octopus genes (*Figure 2-figure supplement 4)*, suggesting that the *Sp8/9* gene underwent a duplication in cephalopod mollusks. Therefore, we designate the octopus *Sp8/9* paralogs as *Sp8/9a* and *Sp8/9b,* and the cuttlefish *Sp8/9* gene that we isolated is the ortholog of *Sp8/9a*.

We next investigated the spatial and temporal expression patterns of these genes during cuttlefish limb development. Genes that pattern the proximodistal axis of arthropod and vertebrate limbs (Lecuit & Cohen, 1997; Mercader et al., 1999; Panganiban et al., 1997; Pueyo & Couso, 2005) showed similarly polarized patterns of expression along the proximodistal axis of cuttlefish limb buds, with *Exd* and *Htx* restricted proximally (*Figure 2B, F and G; Figure 3A-E;* and *Figure 3-figure supplement 1 A and B*) and *Dll*, *Dac*, *Sp8/9a*, *Wnt1, Wnt5,* and *Wnt7* restricted distally (*Figure 2C, H-J*; *Figure 3F-I*; *Figure 3-figure supplement 1 C-E and L-N*). At stages 20-21, the distal expression boundaries of *Exd* and *Htx* and the proximal expression boundaries of *Dll* and *Sp8/9a* appear to mark the morphological boundary between the proximal sucker-free and the distal sucker-forming regions (compare right panels in *Figure 2F-H and J* with *Figure 1P*). Indeed, at stages when arms and tentacles begin to develop their distinctive morphologies -- tentacles are longer and have an extensive proximal sucker-

free domain -- the *Exd*/*Htx* expression domains were found to extend further distally in tentacles (*Figure 3B,D*) compared to arms (*Figure 3A* and *C*). This distal expansion of the *Exd*/*Htx* expression domain matches the expanded sucker-free region and the distal restriction of suckers in tentacles (*Figure 3E*).

Our finding that the proximodistal axis of cuttlefish limbs shares patterns of molecular regionalization with arthropod and vertebrate limbs led us to examine whether anteroposterior and dorsoventral axis development are also conserved. Posteriorly polarized activation of Hedgehog signaling in arthropod and vertebrate limbs is essential for proper patterning of the anteroposterior axis, and ectopic activation of the Hedgehog pathway induces anterior duplication of posterior structures (Basler & Struhl, 1994; Kojima et al., 1994; Riddle et al., 1993). We analyzed *Hh* expression during cuttlefish limb development at stages 16 to 20 and found that *Hh* expression is also polarized to one side of cuttlefish limb buds. In cuttlefishes, however, *Hh* expression is restricted to the anterior margin of the limb bud, whereas in arthropods and vertebrates, *Hh/Shh* is expressed posteriorly (*Figure 2D* and *K*). Consistent with the anterior localization of *Hh*, we detected expression of *Patched,* which serves as a readout of Hedgehog signal transduction, in an anterior-to-posterior gradient (*Figure 2L*). Thus, anteroposteriorly restricted activation of the Hedgehog pathway is a conserved feature of cephalopod, arthropod, and vertebrate limb development, but the polarity of the signaling center is reversed in cephalopod limbs. By stage 21, the anteriorly restricted *Hh* domain has diminished and a new, central expression domain appears in the location of the brachial nerve primordia *(Figure 3-figure supplement 1F,K).*

We then examined the dorsoventral axis, which is controlled by the antagonistic actions of wg/Wnt and dpp/Bmp signaling in arthropods and vertebrates (Brook & Cohen, 1996; Cygan et al., 1997; Diaz-Benjumea et al., 1994; Jiang & Struhl, 1996; Parr & McMahon, 1995). In arthropods, the Wnt ligand *wg* is expressed ventrally, whereas the *Bmp2/4* ortholog *dpp* is expressed dorsally (Basler & Struhl, 1994; Diaz-Benjumea et al., 1994). Expression and function of the Wnt-Bmp network is conserved, albeit with inverted polarity, in vertebrate limbs; *Wnt7a* is expressed dorsally (Parr & McMahon, 1995) and Bmp signaling activates *Engrailed1* (*En1*) ventrally (Ahn et al., 2001), and these interactions regulate development of dorsal and ventral limb structures (Cygan et al., 1997; Parr & McMahon, 1995). During cuttlefish limb development, *Bmp2/4* and *En* show dorsally polarized expression (*Fig 2E, M* and *N*). Genes encoding Wnt ligands (*Wnt1*, *Wnt5* and *Wnt7*) and cellular components of canonical Wnt signaling cascade (*Tcf3/4* and *Frz9/10*) are expressed broadly throughout the dorsoventral axis of cuttlefish limb buds (*Figure 3F-I* and *Figure 3-figure supplement 1L-R*); however, the secreted Wnt antagonists *Notum* and *Sfrp1/2/5* are expressed dorsally in the limb and interlimb regions (*Figure 3J-M*), with the *Sfrp1/2/5* domain extending deeper into the dorsal limb buds (*Figure 2O; Figure 3M*). This dorsal expression of Wnt antagonists suggests a mechanism for restriction of Wnt signaling to the ventral side of the cephalopod limb buds. Taken together, these results suggest that the genetic pathways active along the proximodistal, anteroposterior, and dorsoventral axes of cephalopod limbs are homologous to the networks that regulate limb development in arthropods and vertebrates.

In order to further test this hypothesis, we next performed a series of functional experiments to determine whether polarized expression of these signaling molecules is involved in patterning the anteroposterior and dorsoventral axes of cuttlefish limbs (described below). We developed a method for *ex-ovo* culture of cuttlefish embryos (see Material and Methods) to allow *in vivo* manipulations of genetic pathways in early limb buds,.

Bmp signaling controls dorsoventral patterning of cuttlefish limbs

A hallmark of dorsoventral polarity is the restriction of sucker buds to the ventral surface of the limb (*Figure 1C, D and S*), and this is preceded by ventral expression of *Notum* in the sucker-forming region at stage 21 (*Figure 3N-Q*). We asked whether polarized expression of *Bmp2/4* on the dorsal side of cuttlefish limb buds is required for the specification of dorsal identity. To repress dorsal Bmp activity, we implanted carrier beads loaded with Noggin (Nog), a secreted Bmp inhibitor protein, on the dorsal side of stage 17 limb buds (*Figure 4A*). Implantation of Nog beads to the dorsal side of cuttlefish limb buds resulted in ectopic, dorsal expansion of the *Notum* mRNA domain (n=3/3; control PBS [phosphate buffered saline] beads had no effect on *Notum* expression [n=3/3]) (*Figure 4G,H*). To determine whether inhibition of dorsal Bmp signaling respecifies dorsal cells to form ventral structures, we repeated the experiment and allowed embryos to develop to stage 26-27. Analysis of limb morphology by scanning electron microscopy revealed the presence of ectopic sucker buds on the dorsal surface of Nog-treated limbs (n=8/12; *Figure 4B*; *Figure 4 - figure supplement 1A*

and *B)*. The ectopic dorsal suckers extended around the distal tip of the limb and joined the ventral sucker field. By contrast, in limbs that received control PBS beads dorsally, sucker buds were restricted to ventral surface and terminated at the normal dorsal-ventral boundary at the tip of the limb (n=15/15; *Figure 4C*). Our finding that antagonism of Bmp signaling results in development of ventral structures (sucker buds) on the dorsal side of the limb indicates that dorsal *Bmp2/4* activity is required for the early specification of dorsal identity in cephalopod limb development.

Hedgehog signaling at the anterior margin of cuttlefish limb buds controls anteroposterior patterning of the sucker field

We then investigated whether the mechanism of anteroposterior patterning is conserved between cephalopod and vertebrate/arthropod limbs. To determine whether the anterior expression of *Hh* in cuttlefish limb buds controls anteroposterior patterning, we grafted *Hh*-expressing cells from the thickened funnel epithelium (Tarazona et al., 2016) to the posterior side of stage 17 limb buds, which created an ectopic source of Hh opposite the endogenous *Hh* expression domain (*Figure 4D*). We used *Hh*-expressing cells from the funnel, rather than the anterior side of the limb bud, to exclude the possibility of grafted limb cells undergoing self-differentiation. Approximately ten days after receiving the graft, host limbs developed a posterior limb duplication (n=7/12; *Figure 4E* and *Figure 4 - figure supplement 1C,D*). Analysis of morphology and gene expression revealed that the posterior duplication even contained sucker buds, marked by *Notum* expression (*Figure 4I* and *J*). By contrast, limbs that received control grafts of stage 24

funnel epithelium that lacks *Hh* expression (Tarazona et al., 2016) developed normally (n=8/8; *Figure 4F*).

Although these results suggest that *Hh* is sufficient to re-specify anteroposterior polarity in cuttlefish limbs, we wanted to exclude the possibility that posterior identity was induced by other factors that could be present in the graft. Therefore, we tested whether Hh signaling is necessary for anteroposterior patterning of cephalopod limbs by specifically repressing endogenous Hh signaling. A notable morphological feature of cephalopod limbs is the anteroposterior arrangement of parallel sucker rows on the ventral surface (*Figure 1C, D* and *S*). Based on the results of the transplantation experiments, we reasoned that Hh signaling could regulate the number of sucker rows along the anteroposterior axis of cephalopod limbs, similar to the manner in which Hh specifies digit number along the anteroposterior axis of vertebrate limbs (Lewis et al., 2001; Scherz et al., 2007; Zhu et al., 2008).

Transitory treatment (2 days) of cuttlefish embryos at stage 16, when *Hh* is first expressed on the anterior side of the early limb bud, with the small molecule cyclopamine, an inhibitor of Smoothened that represses Hh signaling (*Figure 4K*), disrupted the anteroposterior distribution of sucker rows in arms and tentacles. Severity of this phenotype ranged from arms with a reduced number of suckers and sucker rows (n=10/10; *Figure 4N* and *O*) to completely sucker-free tentacles (n=8/10*; Figs. 4L*). Control treatments with vehicle only (DMSO) did not alter the normal anteroposterior pattern of sucker rows (n=8/8; *Figure 4M* and *P*). Finally, to confirm that the phenotype

of cyclopamine-treated embryos was not due to failure in brachial nerve differentiation, we examined acetylated tubulin immunofluorescence, which shows that the brachial nerve cords develop in both cyclopamine and DMSO treated embryos (*Figure 4 - figure supplement 1E,F*). These results show that Hh signaling is necessary for proper patterning of the anteroposterior axis in cephalopod limb development.

Discussion

Our finding that the proximodistal, dorsoventral, and anteroposterior axes of cuttlefish limb buds are patterned by the same pathways that regulate arthropod and vertebrate limb development suggests that the independent evolution of limbs in cephalopod mollusks involved recruitment of an ancient genetic program for appendage development. Discovery of this appendage developmental circuit within Spiralia demonstrates its deep conservation across all three branches of Bilateria (i.e., Deuterostomia, Ecdysozoa and Spiralia), suggesting its presence in the common ancestor of all bilaterians. Parallel recruitment of this ancient developmental genetic program may have played a role in the independent evolution of a wide diversity of appendages in many bilaterian lineages (Moczek & Nagy, 2005; Shubin et al., 2009).

Examination of gene expression in lateral parapodial appendages of the polychaete worm *Neanthes,* also a Spiralian*,* led to the suggestion that the molecular mechanisms of appendage development might not be conserved with ecdysozoans and deuterostomes (Winchell & Jacobs, 2013; Winchell et al., 2010). The finding that cephalopod, arthropod, and vertebrate appendages develop using conserved

developmental mechanisms does not exclude the possibilty that other types of appendages evolved by recruiting a different set of developmental tools (or by utilizing the same tools but in different patterns).. However, given that very few genes have been examined in *Neanthes* parapodia, it is difficult to conclude whether the reported differences between parapodia and arthropod/vertebrate/cephalopod limbs reflect the unique nature of parapodia or lineage-specific divergences that occurred after recruitment of the core developmental program. How parapodia fit into the picture of animal appendage evolution will require additional studies of spiralian appendages that increase the diversity of species, types of appendages, and number of genes/pathways interrogated. Nonetheless, our discovery that cephalopod arms and tentacles evolved by parallel recruitment of the same genetic program that orchestrates appendage formation in arthropods and vertebrates suggests that this program was present in the Bilaterian common ancestor.

Although cephalopod arms and tentacles do not share a direct homologous structure outside cephalopoda, developmentally they likely originated from the ventral embryonic foot, one of the morphological and embryological hallmarks of the molluscan bodyplan (Nödl et al., 2016). Therefore, cephalopod arms and tentacles can be considered evolutionary novelties that are derived from a structure that is conserved across Mollusca. This raises the question of whether other foot-derived outgrowths/appendages (e.g. in sea slugs) evolved by co-opting the same limb developmental program that cephalopods, arthropods and vertebrates use to construct their appendages.

Whereas conservation of this ancient developmental program was probably central to the origin of cephalopod limbs, the results presented here also indicate that fine-scale regulatory changes may have played a role in the diversification of cephalopod limb morphologies. For example, our data suggest that evolution of tentacles from serially homologous arms may have resulted from a distal shift in the expression of proximal identity genes, such as *Exd* and *Htx,* which could have produced an extensive proximal sucker-free domain and restricted suckers to a distal pad. Likewise, the results of functional manipulations of Hh signaling in cuttlefish limbs raise the possibilty that the diversity in sucker row number along the anteroposterior axis displayed by different cephalopod lineages (i.e. four rows in squids and cuttlefishes, two in octopus and one in vampire squid and glass octopus) could be explained by modulation of Hh signaling, in the same way that gradual changes to *Shh* regulation has led to variation in digit number in tetrapod vertebrates (Scherz et al., 2007; Shapiro et al., 2003; Zhu et al., 2008).

Finally, we note that while the data presented here point to the existence of a deeply conserved genetic program for appendage development across *Bilateria*, this does not imply that the limbs of cephalopods, arthropods, and vertebrates are homologous structures or that limbs were present in the common ancestor. Rather, these results show that homologous developmental mechanisms underlie the multiple origins of bilaterian limbs.

Materials and Methods

No statistical methods were used to predetermine sample size. Embryos were randomized in each experiment. The investigators were not blinded to allocation during experiments and outcome assessment.

Embryo collection and preparation

Sepia officinalis eggs were purchased from commercial suppliers, incubated until they reached the required stages (Lemaire, 1970), and prepared for *in situ* hybridization (ISH) and immunohistochemistry as described (Tarazona et al., 2016).

Optical projection tomography (OPT)

Three-dimensional reconstructions of gene expression in cuttlefish embryos were performed as previously described (Tarazona et al., 2016).

Scanning electron microscopy

Cuttlefish embryos were fixed in 4% paraformaldehyde in phosphate buffered saline (PBS) overnight at 4°C and were washed with PBS the next day. Embryos were fixed in 1% osmium tetroxide solution in PBS for 30 minutes and then washed three times in PBS, dehydrated through a graded ethanol series, critical point dried, and sputter coated with gold. Embryonic samples were scanned using a Hitachi SU5000 and Hitachi TM3000.

Gene cloning and molecular phylogenetic analysis

RNA extraction from *Sepia* embryos at stages 15–26 was performed using TRIzol reagent (Ambion) following the manufacturer's instructions. cDNA synthesis was performed by an AMV reverse transcriptase (New England Biolabs) following the manufacturer's instructions. PCR amplification was carried out on *Sepia* cDNA pools, amplicons were cloned into TA vectors and sequenced. We then performed multiple sequence alignments (MSA) with ClustalW (PMID: 7984417) using the predicted amino acid sequence of our cuttlefish cDNA fragments, and putative metazoan orthologous

genes downloaded from NCBI RefSeq protein databases (Figure 1-Supplementary file 1). We performed nine MSA for Wnt, Tcf, Sfrp, Notum, Patch, Hh, Bmp, Sp and Homeodomain families. Each of the nine MSA was analyzed by ProtTest (PMID: 15647292), in order to determine the best combination of amino acid substitution model and other free parameters (amino acid site frequency, site heterogeneity and invariant sites), using Akaike information criterion (Figure 1-Supplementary file 1). We applied the best model in RaXML (PMID: 18853362) for each MSA and performed maximum likelihood phylogenetic inference, estimating branch support by bootstrap, and then majority consensus of the trees from all bootstrap partitions was performed to compute the final tree topology.

In situ hybridization (ISH) and immunohistochemistry

Whole-mount ISH was performed using digoxigenin and fluorescein labeled antisense (or sense control) RNA probes according to protocols previously described (Tarazona et al., 2016). Proliferating cells were detected by immunolocalization of Histone H3 Serine 10 phosphorylation using an antibody against H3S10p/PHH3 (06-570, EMD Millipore) and brachial nerve tissue was detected using an antibody against acetylated alpha tubulin (ab24610, Abcam).

Cuttlefish _ex-ovo_ embryo culture and embryo manipulations

A protocol for *ex-ovo* cuttlefish embryo culture was established for this study, as a modified version of previous descriptions of *ex-ovo* embryo culture in squid (Arnold, 1990). Briefly, to minimize the problem of bacterial and fungal contamination we started the protocol by taking 10 cuttlefish eggs at the appropriate stage, placing them in a 50ml tube, and washing them with 0.22 µm filtered artificial sea water (FASW) five times. Eggs were then cleaned with a freshly prepared 5% bleach solution (0.25% sodium hypochlorite in FASW) for 5 seconds and immediately washed with FASW five times. The bleaching and washing steps were repeated two to three times. Five additional washes with FASW were carried out before incubating the eggs in 2X antibiotic/antimycotic solution (A5955, Sigma) in FASW for 2 hours at ambient temperature.

Each cuttlefish egg was then transferred to a 50 mm diameter petri dish that was coated with a ~ 5mm layer of 0.5% low melting point agarose (16520050, ThermoFisher), and filled with culture medium (components described below). The agarose layer had a hemispherical depression in the center of the dish made with a sterile 10 mm acrylic necklace bead before gel solidification. The 10mm hemispherical depression is essential to maintain the normal shape of the yolk mass once the embryos are outside their egg case. Embryos were then extracted from their egg cases (*S. officinalis* are housed individually, one embryo per egg case) very slowly and with extreme care to avoid rupturing the yolk mass at the vegetal pole of the egg and were carefully placed in the hemispherical depression in the agarose. To extract the embryo, a single 5mm diameter hole was created in the egg case, which generates a burst of the vitelline liquid and part of the embryo out from the egg case. With the hole kept open, the spontaneous shrinkage of the egg case aided in the expelling of the large cuttlefish embryo. Of every ten eggs prepared this way, between two and five embryos were damaged and had to be discarded. Embryos were cultured at 17°C.

Protein carrier beads and tissue grafting

For protein carrier bead implantation, 150µm diameter Affi-Gel Blue Gel beads (153-7301, Biorad) were selected and transferred to 1mg/ml recombinant human Noggin protein (6057-NG, R&D Systems) in PBS and incubated for 30 minutes to 1 hour at ambient temperature before being implanted in embryos. Control beads were incubated in PBS only.

Grafts with *Hh*-expressing tissue were performed by taking stage 24 donor embryos and carefully dissecting the funnel side of the mantle-funnel locking system, which carries the *Hh*-expressing thickened funnel epithelium (Tarazona et al., 2016). The dissected tissue was transferred to 10 mg/ml Dispase II (D4693, Sigma) in cuttlefish culture medium and incubated for 40 minutes or until the thickened epithelium was easily detaching from the underlying mesenchyme with the aid of forceps. Tissue was then transferred to cuttlefish culture medium without Dispase II until they were grafted into

limb buds of stage 17 host embryos. Control grafts were performed using the non-*Hh* expressing epithelium of the funnel.

After bead implantation or tissue grafts, embryos were incubated at 17°C until control embryos reached stage 26, at which point all embryos were collected and prepared for SEM or ISH.

Cuttlefish culture medium

We used a modified version of a cell culture medium for squid neuron, glia and muscle cells that was previously described (Rice et al., 1990). Cuttlefish culture medium had no glucose, was buffered with 20mM HEPES and adjusted the pH to 7.6. The medium contained: 430 mM NaCl, 10 mM KCl, 10 mM CaCl2, 50 mM MgCl2, 1X MEM Non-Essential Amino Acids Solution (11140-076, Life Technologies), 1X MEM Amino Acids Solution (11130-051, Life Technologies), 1X MEM Vitamin Solution (11120-052, Life Technologies), 2 mM L-Glutamine (25030-081, Life Technologies). The medium was supplemented with 20% heat inactivated fetal bovine serum (16000044, ThermoFisher) and 1X antibiotic/antimycotic solution (A5955, Sigma).

Treatments with small-molecule inhibitors

Cyclopamine treatments were performed as described previously (Tarazona et al., 2016) with the following modifications; stage 16 embryos were treated with 10 μM cyclopamine (C988400, Toronto Research Chemicals) for 2 days, then washed thoroughly ten times with FASW. Embryos were then washed 5 more times every hour and one time every day before collecting the embryos for SEM. Control embryos were treated with 0.1% DMSO and then washed as described above.

Acknowledgments

We thank Emily Merton for technical support, Karen L. Kelley and Kimberly L. Backer-Kelley (UF ICBR) for assistance with electron microscopy, and members of our

laboratory for helpful comments and discussions. O.A.T. was supported by a Howard Hughes Medical Institute International Student Research Fellowship, D.H.L. by a Society for Developmental Biology “Choose Development!” fellowship, and L.A.S. by an EDEN Undergraduate Internship.

Funding

This project was supported by an award from the Howard Hughes Medical Institute (to M.J.C).

Competing Interests

The authors declare no competing or financial interests.

Author Contributions

O.A.T. and M.J.C. designed the experiments, analyzed the data and wrote the paper. All authors collaborated in reviewing and editing the paper. O.A.T., D.H.L. and L.A.S. cloned the *Sepia* genes and analyzed gene and protein expression. O.A.T. performed the molecular phylogenetic analyses, scanning electron microscopy, optical projection tomography scanning, three-dimensional reconstructions, *ex-ovo* embryo culture, bead implantation, tissue grafting, and small-molecule treatments.

Supplementary Materials

Figure 1 - figure supplement 1;

Figure 1 - Supplementary Movies 1 to 5

Figure 2 - figure supplements 1 to 10

Figure 2 - Supplementary file 1

Figure 3 - figure supplement 1

Figure 4 - figure supplement 1

References

Ahn, K., Mishina, Y., Hanks, M. C., Behringer, R. R., & Crenshaw, E. B., 3rd. (2001). BMPR-IA signaling is required for the formation of the apical ectodermal ridge and dorsal-ventral patterning of the limb. *Development, 128*(22), 4449-4461.

Arnold, J. M. (1965). Normal Embryonic Stages of the Squid, Loligo pealii (Lesueur). *Biological Bulletin, 128*(1), 24-32.

Arnold, J. M. (1990). Embryonic Development of the Squid. In W. J. Adelman, J.M. Arnold, & D.L. Gilbert (Eds.), *Squid as Experimental Animals*: Springer US.

Basler, K., & Struhl, G. (1994). Compartment boundaries and the control of Drosophila limb pattern by hedgehog protein. *Nature, 368*(6468), 208-214.

Brook, W. J., & Cohen, S. M. (1996). Antagonistic interactions between wingless and decapentaplegic responsible for dorsal-ventral pattern in the Drosophila Leg. *Science, 273*(5280), 1373-1377.

Cygan, J.A., Johnson, R.L., & McMahon, A.P. (1997). Novel regulatory interactions revealed by studies of murine limb pattern in Wnt-7a and En-1 mutants. *Development, 124*(24), 5021-5032.

Diaz-Benjumea, F. J., Cohen, B., & Cohen, S. M. (1994). Cell interaction between compartments establishes the proximal-distal axis of Drosophila legs. *Nature, 372*(6502), 175-179.

Grimaldi, A., Tettamanti, G., Acquati, F., Bossi, E., Guidali, M. L. , Banfi, S., . . . de Eguileor, M. (2008). A hedgehog homolog is involved in muscle formation and organization of Sepia officinalis (mollusca) mantle. *Dev Dyn, 237*(3), 659-671. doi:10.1002/dvdy.21453

Jiang, J., & Struhl, G. (1996). Complementary and Mutually Exclusive Activities of Decapentaplegic and Wingless Organize Axial Patterning during Drosophila Leg Development. *Cell, 86*(3), 401-409.

Kojima, T., Michiue, T., Orihara, M., & Saigo, K. (1994). Induction of a mirror-image duplication of anterior wing structures by localized hedgehog expression in the anterior compartment of Drosophila melanogaster wing imaginal discs. *Gene, 148*(2), 211-217.

Kroger, B., Vinther, J., & Fuchs, D. (2011). Cephalopod origin and evolution: A congruent picture emerging from fossils, development and molecules. *Bioessays, 33*(8), 602-613.

Lecuit, T., & Cohen, S. M. (1997). Proximal-distal axis formation in the Drosophila leg. *Nature, 388*(6638), 139-145.

Lee, P. N., Callaerts, P., de Couet, H. G., & Martindale, M. Q. (2003). Cephalopod Hox genes and the origin of morphological novelties. *Nature, 424*(6952), 1061-1065.

Lemaire, J. . (1970). Table de developpement embryonnaire de Sepia officinalis. L. (Mollusque Cephalopode). *Bull Soc Zool France*(95), 95:773–782. .

Lewis, P. M., Dunn, M. P., McMahon, J. A., Logan, M., Martin, J. F., St-Jacques, B., & McMahon, A. P. (2001). Cholesterol modification of sonic hedgehog is required for long-range signaling activity and effective modulation of signaling by Ptc1. *Cell, 105*(5), 599-612.

Mercader, N., Leonardo, E., Azpiazu, N., Serrano, A., Morata, G., Martinez-A, C., & Torres, M. (1999). Conserved regulation of proximodistal limb axis development by Meis1/Hth. *Nature, 402*(6760), 425-429.

Minelli, A. (2000). Limbs and tail as evolutionarily diverging duplicates of the main body axis. *Evol Dev, 2*(3), 157-165.

Minelli, A. (2003). *The Development of Animal Form: Ontogeny, Morphology, and Evolution*: Cambridge University Press.

Moczek, A. P., & Nagy, L. M. (2005). Diverse developmental mechanisms contribute to different levels of diversity in horned beetles. *Evol Dev, 7*(3), 175-185. doi:10.1111/j.1525-142X.2005.05020.x

Nielsen, C. (2012). *Animal Evolution: Interrelationships of the Living Phyla*: OUP Oxford.

Nödl, M. T., Kerbl, A., Walzl, M. G., Müller, G. B., & de Couet, H. G. (2016). The cephalopod arm crown: appendage formation and differentiation in the Hawaiian bobtail squid Euprymna scolopes. *Front Zool, 13*, 44. doi:10.1186/s12983-016-0175-8

Panganiban, G., Irvine, S. M., Lowe, C., Roehl, H., Corley, L. S., Sherbon, B., . . . Carroll, S. B. (1997). The origin and evolution of animal appendages. *Proc Natl Acad Sci U S A, 94*(10), 5162-5166.

Parr, B. A., & McMahon, A. P. (1995). Dorsalizing signal Wnt-7a required for normal polarity of D-V and A-P axes of mouse limb. *Nature, 374*(6520), 350-353. doi:10.1038/374350a0

Prpic, N. M. (2008). Parasegmental appendage allocation in annelids and arthropods and the homology of parapodia and arthropodia. *Front Zool, 5*, 17. doi:10.1186/1742-9994-5-17

Pueyo, J. I., & Couso, J. P. (2005). Parallels between the proximal-distal development of vertebrate and arthropod appendages: homology without an ancestor? *Curr Opin Genet Dev, 15*(4), 439-446.

Rice, R.V., Mueller, R., & Adelman, W.J. (1990). Tissue culture of squid neurons, glia, and muscle cells. In W. J. Adelman, J.M. Arnold, & D.L. Gilbert (Eds.), *Squids as experimental animals.*: Springer US.

Riddle, R. D., Johnson, R. L., Laufer, E., & Tabin, C. (1993). Sonic hedgehog mediates the polarizing activity of the ZPA. *Cell, 75*(7), 1401-1416.

Ruppert, E.E., Fox, R.S., & Barnes, R.D. (2004). *Invertebrate Zoology: A Functional Evolutionary Approach*: Thomson-Brooks/Cole.

Scherz, P. J., McGlinn, E., Nissim, S., & Tabin, C. J. (2007). Extended exposure to Sonic hedgehog is required for patterning the posterior digits of the vertebrate limb. *Developmental biology, 308*(2), 343-354.

Shapiro, M. D., Hanken, J., & Rosenthal, N. (2003). Developmental basis of evolutionary digit loss in the Australian lizard Hemiergis. *J Exp Zool B Mol Dev Evol, 297*(1), 48-56.

Shigeno, S., Sasaki, T., Moritaki, T., Kasugai, T., Vecchione, M., & Agata, K. (2008). Evolution of the cephalopod head complex by assembly of multiple molluscan body parts: Evidence from Nautilus embryonic development. *J Morphol, 269*(1), 1-17.

Shubin, N., Tabin, C., & Carroll, S. (1997). Fossils, genes and the evolution of animal limbs. *Nature, 388*(6643), 639-648.

Shubin, N., Tabin, C., & Carroll, S. (2009). Deep homology and the origins of evolutionary novelty. *Nature, 457*(7231), 818-823. doi:10.1038/nature07891

Smith, S. A., Wilson, N. G., Goetz, F. E., Feehery, C., Andrade, S. C., Rouse, G. W., . . . Dunn, C. W. (2011). Resolving the evolutionary relationships of molluscs with phylogenomic tools. *Nature, 480*(7377), 364-367.

Tabin, C. J., Carroll, S. B., & Panganiban, G. (1999). Out on a Limb: Parallels in Vertebrate and Invertebrate Limb Patterning and the Origin of Appendages. *American Zoologist, 39*(3), 650-663.

Tarazona, O. A., Slota, L. A., Lopez, D. H., Zhang, G., & Cohn, M. J. (2016). The genetic program for cartilage development has deep homology within Bilateria. *Nature, 533*(7601), 86-89. doi:10.1038/nature17398

Winchell, C. J., & Jacobs, D. K. (2013). Expression of the Lhx genes apterous and lim1 in an errant polychaete: implications for bilaterian appendage evolution, neural development, and muscle diversification. *Evodevo, 4*(1), 4. doi:10.1186/2041-9139-4-4

Winchell, C. J., Valencia, J. E., & Jacobs, D. K. (2010). Expression of Distal-less, dachshund, and optomotor blind in Neanthes arenaceodentata (Annelida, Nereididae) does not support homology of appendage-forming mechanisms across the Bilateria. *Dev Genes Evol, 220*(9-10), 275-295. doi:10.1007/s00427-010-0346-0

Zhu, J., Nakamura, E., Nguyen, M. T., Bao, X., Akiyama, H., & Mackem, S. (2008). Uncoupling Sonic hedgehog control of pattern and expansion of the developing limb bud. *Dev Cell, 14*(4), 624-632.

Figure Legends

Figure 1. Development of arms and tentacles in the cuttlefish, *Sepia officinalis*. (**A**) Phylogenetic relationships of Mollusca based on phylogenomic data (Smith et al., 2011) illustrating the unique morphology of the cephalopod body plan compared to other mollusks. (**B**) OPT reconstruction of a cuttlefish hatchling showing positions of the limbs; only arms are visible (see also Supplementary Movie 1). (**C** to **D**), SEM of the ventral side of a cuttlefish arm (C) and tentacle (D). Suckers are pseudocolored blue. Note distal restriction of suckers in tentacle relative to arm. (**E**) OPT reconstruction illustrating the internally retracted tentacles. Specimens are same as in (B), but here the tentacles are displayed in orange and the rest of the tissue is rendered translucent (see also Supplementary Movie 2). (**F** and **G**) Phospho-histone H3 (PHH3) immunostaining at stage 15 shows localized clusters of proliferating cells at the onset of limb development (black arrowheads) but little proliferation in the interlimb region (open arrowhead). Colorimetric detection with DAB in a whole mount in (F) and immunofluorescence on limb cryosections (white bracket) in (G). (**H** and **L**) OPT reconstructions of cuttlefish embryos at stages 16 to 24. Cuttlefishes have five bilaterally symmetric limb pairs (ten limbs; eighth arms and two tentacles). Numbered arrowheads mark all five limbs/limb buds on the left side of each embryo. The left tentacle differentiates from position number four (orange arrowhead), whereas arms form from limb buds at the other positions (yellow arrowheads). See also Supplementary Movies 3-5. A, anterior; P, posterior; D, dorsal; V, ventral; Stm, stomodeum; Mnt, mantle. (**M** to **O**) SEM during early stages of cuttlefish limb development (stages 16 to 19). Morphogenesis of the limb is first observed as a slight swelling (M) that transforms into a limb bud (O) as proximodistal outgrowth progresses. D, dorsal; V, ventral. **p-s**, SEM at later stages of cuttlefish limb development (stages 21 to 25) showing the formation of sucker buds on the ventral surface of a developing limb. A primordial sucker band (yellow arrows) is observed along the ventral midline of a stage 21 limb bud (P). At later stages, the band cleaves superficially from the proximal end to form the sucker buds (pseudocolored blue in Q to S). Scale bars: 0.5 mm (C and D) and 100 µm (M to S).

Figure 2. Molecular regionalization of proximodistal, anteroposterior, and dorsovental axes during cephalopod limb development. (**A**) OPT reconstruction of cuttlefish embryo at stage 20 showing all five limb buds on the left side of the embryo (arms, yellow arrowheads; tentacle, orange arrowhead). (**B** to **E**) OPT reconstructions showing four representative genes with polarized expression patterns along major axes of limb buds (gene expression indicated by orange/yellow). Proximodistally polarized expression of *Exd* (B) and *Wnt5* (C). Anteroposteriorly polarized expression of *Hh* (D**),** dorsoventrally polarized expression of *Bmp2/4* (E). (**F** to **O**), *In situ* hybridizations of cuttlefish limb buds at stage 17 (left) and stage 20 (right) showing polarized patterns of expression along the proximodistal axis for *Exd* (F), *Htx* (G), *Dll* (H), *Dac* (I) and *Sp8/9* (J); the anteroposterior axis for *Hh* (K) and *Ptc* (L); and the dorsoventral axis for *Bmp2/4* (M), *En* (N) and *Sfrp1/2/5* (O). A, anterior; P, posterior; D, dorsal; V, ventral; Di, distal; Pr, proximal.

Figure 3. Expression of proximal identity genes *Exd* and *Htx* in arms and tentacles corresponds with distribution of suckers; Wnt signaling repressors are dorsally restricted. (A and **B**) Compared to arms (A), tentacles (B) show a distally expanded domain of *Exd* expression in the proximal region of the limb. (**C** and **D**) A similar pattern of expression is detected for *Htx* during arm (C) and tentacle (D) development. Distal boundary of *Exd* and *Htx* expression marked by black arrowheads in (A to D). (**E**) Expanded expression of proximal identity genes correlates with the expanded sucker-free domain seen in tentacles compared to arms. (**F** and **H**) The Wnt ligands *Wnt1*, *Wnt5* and *Wnt7* show a distally restricted expression but no dorsoventral polarization at stages 17 and 20. (**I**) The Wnt signaling transcription factor *Tcf3/4* is also distally restricted but shows no dorsoventral polarization at stages 17 and 20. (**J** and **K)** Fluorescent nuclear stain SYBR Safe highlights limb buds (yellow arrowheads). Boxed region in (J) is enlarged in (K); white arrowhead marks interlimb region. (**L** and **M**) The Wnt ligand repressors *Notum* and *Sfrp1/2/5* are expressed in the dorsal interlimb region (black arrowhead in L and M; compare with K). *Sfrp1/2/5* expression expands into the dorsal limb bud (black arrows in M) in stage 19 embryos, whereas *Notum* stays dorsal

but proximally restricted (open arrowheads mark the limb buds in L). (**N** and **O**) The earliest sign of sucker formation can be detected by SEM as a slight swelling (N) and by *Notum* expression (O) on the ventral side of stage 21 limb buds. (**P** and **Q)** Expression of *Notum* is maintained through later stages of sucker morphogenesis, as seen in stage 26 tentacles (lateral views).

Figure 4. Bmp signaling controls dorsoventral patterning and Hh signaling regulates anteroposterior patterning of cuttlefish limbs. (**A** to **C**) Implantation of carrier beads loaded with the Bmp inhibitor Noggin (A) results in formation of ectopic sucker buds (n=8/12) on the dorsal surface of the limb (B), whereas PBS control beads (n=15/15) result in normal development of the dorsal limb (pseudocolored red) restriction of suckers (pseudocolored blue) to the vental side of the limb (C). (**D** to **F**), *Hh*-expressing cells (taken from the funnel of a stage 24 donor embryo) grafted to the posterior side of a stage 17 cuttlefish limb bud (D) generates a posterior mirror-image limb duplication (n=7/12; yellow arrow in E), whereas no duplication (n=8/8) results when control (Hh-negative) cells are grafted to the same position (F). Sucker buds are pseudocolored blue in (E and F); sucker buds in duplicated limb marked with a white arrowhead. (**G** and **H**) Noggin beads induce ectopic expression of *Notum* on the dorsal side of the limb (G). Limbs receiving control PBS beads show normal expression of *Notum* ventrally (H). (**I** and **J**) Graft of *Hh*-expressing tissue to the posterior side of the limb induces ectopic domain of *Notum* prior to duplication of the limb (I; black arrowhead). Note the two separate domains of *Notum* expression in I compared to a single *Notum* expression domain in the limb with the *Hh*-negative control graft (J). (**K** to **P**) Transitory repression of Hh signaling by cyclopamine (K) during early stages of limb development disrupts the anteroposterior distribution of sucker bud rows (L, N, O). Cyclopamine-treated limbs showing complete loss of suckers in tentacles (L) and reduction in the number of sucker bud rows in arms (N and O). Control embryos treated with vehicle only (DMSO) develop the normal number of sucker bud rows in tentacles (M) and arms (P). Sucker buds are pseudocolored blue in (B, E, F, and M- P). Scale bars 100 μm.

Legends to Figure Supplements

Figure 1 – figure supplement 1. Sucker morphogenesis. All panels show scanning electron micrographs; scale bars, 100 µm. (**A** and **B**) Sucker buds are arranged in parallel rows along the anteroposterior axis, with four rows in arms (A) and eight rows in tentacles (B). (**C** to **G**) Sucker formation progresses from distal to proximal. Colored squares in c are shown at higher magnification in d-g. Superficial cleavage of the proximal side of the primordial sucker band in (D) and segregation of the recently formed sucker buds in (E). Early sucker bud cells (G) form a dome-shaped outline compared to the rather flattened morphology of the non-sucker forming surface epithelium (F). (**H** and **I**) Higher magnification of sucker buds in a cuttlefish hatchling showing that sucker differentiation is not yet complete in hatchlings (H) compared to the differentiated suckers found in more mature individuals (I), which indicates that a substantial portion of sucker development occurs during post hatchling development.

Figure 1- supplementary movie 1. OPT 3D reconstruction showing cuttlefish hatchling morphology.

Figure 1- supplementary movie 2. OPT 3D reconstruction showing the internal location of the tentacles in a cuttlefish hatchling. Tentacles in orange, other parts of the body in gray (partially translucent).

Figure 1- supplementary movie 3. OPT 3D reconstruction showing morphology of a cuttlefish embryo at stage 17. Embryo is positioned on top of the yolk. The early limb buds (8 arm buds and 2 tentacle buds) can be seen around the margin of the embryo.

Figure 1- supplementary movie 4. OPT 3D reconstruction showing morphology of a cuttlefish embryo at late stage 19.

Figure 1- supplementary movie 5. OPT 3D reconstruction showing the morphology of a cuttlefish embryo at stage 24.

Figure 2 – figure supplement 1. Molecular phylogenetic reconstruction using maximum likelihood implemented in RAxML of *Wnt* family ligands isolated in this study. Arrows mark the phylogenetic placement of 4 cuttlefish *Wnt* sequences.

Figure 2 – figure supplement 2. Molecular phylogenetic reconstruction using maximum likelihood implemented in RAxML of *Pan*/*Tcf* transcription factors isolated in this study. The arrow marks the phylogenetic placement of one cuttlefish *Tcf* sequences.

Figure 2 – figure supplement 3. Molecular phylogenetic reconstruction using maximum likelihood implemented in RAxML of *Dac/Dach* transcription factors isolated in this study. The arrow marks the phylogenetic placement of one cuttlefish *Dac* sequences.

Figure 2– figure supplement 4. Molecular phylogenetic reconstruction using maximum likelihood implemented in RAxML of *Sp* family of transcription factors isolated in this study. The arrow marks the phylogenetic placement of one cuttlefish *Sp* sequence.

Figure 2 – figure supplement 5. Molecular phylogenetic reconstruction using maximum likelihood implemented in RAxML of Homeodomain family of transcription factors isolated in this study. Arrows mark the phylogenetic placement of 4 cuttlefish Homeodomain sequences.

Figure 2 – figure supplement 6. Molecular phylogenetic reconstruction using maximum likelihood implemented in RAxML of *Notum* Wnt inhibitors isolated in this study. The arrow marks the phylogenetic placement of one cuttlefish *Notum* sequence.

Figure 2 – figure supplement 7. Molecular phylogenetic reconstruction using maximum likelihood implemented in RAxML of *Frizzled* Wnt co-receptors and *Sfrp* extracellular Wnt repressors isolated in this study. Arrows mark the phylogenetic placement of one cuttlefish *Frizzled* and one *Sfrp***.**

Figure 2 – figure supplement 8. Molecular phylogenetic reconstruction using maximum likelihood implemented in RAxML of *Tgfβ* family ligands isolated in this study. The arrow marks the phylogenetic placement of cuttlefish *Bmp2/4***.**

Figure 2 – figure supplement 9. Molecular phylogenetic reconstruction using maximum likelihood implemented in RAxML of *Hh* ligand previously isolated (PMID:27111511) in this study. The arrow marks the phylogenetic placement of cuttlefish *Hh* sequence**.**

Figure 2 – figure supplement 10**.** Molecular phylogenetic reconstruction using maximum likelihood implemented in RAxML of Hedgehog *Patch* receptors isolated in this study. The arrow marks the phylogenetic placement of cuttlefish *Patched*.

Figure 3 – figure supplement 1**. Expression of developmental control genes in cuttlefish limb buds.** (**A** to **O**) *In situ* hybridizations showing *Wnt1*, *Wnt5*, *Wnt7*, *Tcf*, *Exd*, *Htx*, *Dll*, *Dac*, *Sp8*, *Hh*, *Ptc*, *Bmp2*/4, *En* and *Sfrp1/2/5* in stage 21 embryos*. Hh* expression in stage 21 limb buds, detected by *in situ* hybridizations in whole mount (F) and cryosections (K) showing the central expression in the brachial nerve cell precursors. (**P** to **R**) *In situ* hybridizations of *Frz9/10* at stages 17 (P and S), 20 (Q and T) and 21(R and U). A, anterior; P, posterior; D, dorsal; V, ventral.

Figure 4 – figure supplement 1**. Sucker development after manipulations of Bmp and Hh signaling pathways.** (**a**) SEM of Noggin-treated limbs shows dorsal ectopic sucker buds (A) as seen in Fig. 4b. (**b**) Higher magnification of the region inside the

yellow square in (A) showing the superficial dome-shape morphology of sucker bud cells. (**C**) SEM of posterior mirror-image duplicated limb caused by graft of *Hh*-expressing tissue, as seen in (Fig. 4e). (**D**) Higher magnification of the region inside the yellow square in (C) shows the superficial dome-shape morphology of sucker bud cells. (**E** and **F**) Differentiation of brachial nerves in cyclopamine-treated (E) and DMSO control (F) embryos revealed by acetylated tubulin in the center of the limbs. Scale bars, 100 μm.

Figure 1

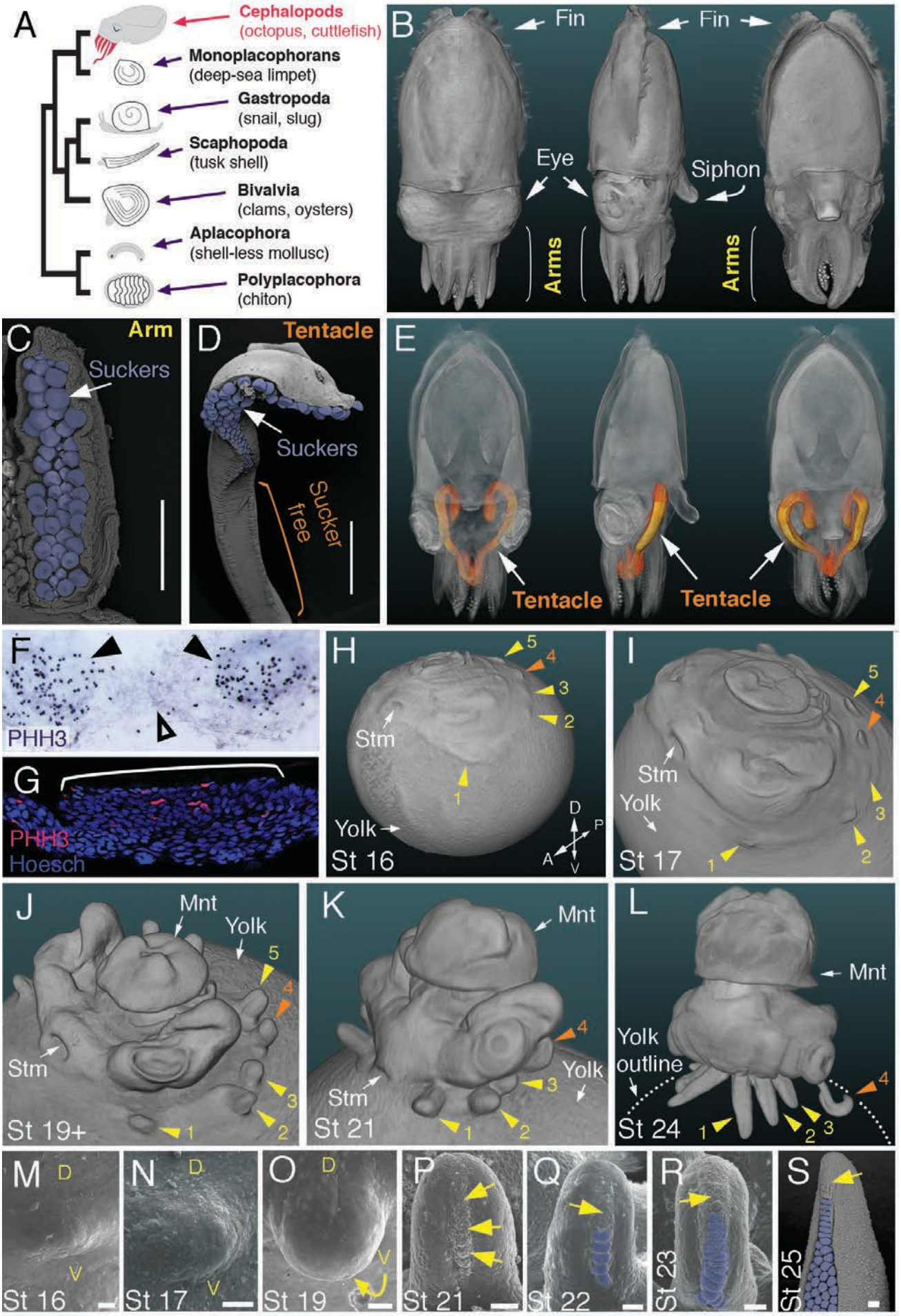
A
Cephalopods
(octopus, cuttlefish)
Monoplacophorans
(deep-sea limpet)
Gastropoda
(snail, slug)
Scaphopoda
(tusk shell)
Bivalvia
(clams, oysters)
Aplacophora
(shell-less mollusc)
Polyplacophora
(chiton)
B
Fin
Fin
Eye
Siphon
Arms
Arms
C
Arm
Suckers
D
Tentacle
Suckers
Sucker free
E
Tentacle
Tentacle
F
PHH3
G
PHH3
Hoesch
H
Stm
Yolk
St 16
I
Stm
Yolk
St 17
J
Mnt
Yolk
Stm
St 19+
K
Mnt
Yolk
Stm
St 21
L
Mnt
Yolk outline
St 24
M
St 16
N
St 17
O
St 19
P
St 21
Q
St 22
R
St 23
S
St 25

Figure 2

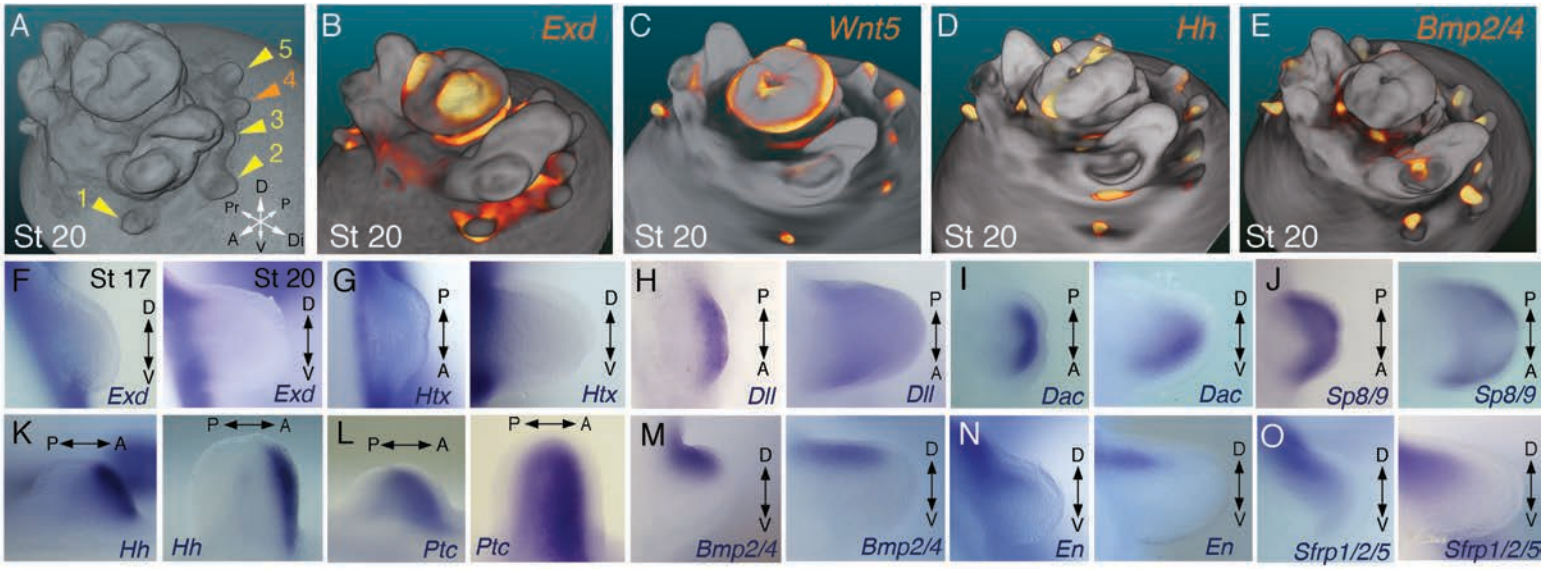
A
5
4
3
2
1
D
Pr
P
A
V
Di
St 20
B
Exd
St 20
C
Wnt5
St 20
D
Hh
St 20
E
Bmp2/4
St 20
F
St 17
D
V
Exd
St 20
D
V
Exd
G
P
A
Htx
D
V
Htx
H
P
A
Dll
P
A
Dll
I
P
A
Dac
D
V
Dac
J
P
A
Sp8/9
P
A
Sp8/9
K
P
A
Hh
P
A
Hh
L
P
A
Ptc
P
A
Ptc
M
D
V
Bmp2/4
D
V
Bmp2/4
N
D
V
En
D
V
En
O
D
V
Sfrp1/2/5
D
V
Sfrp1/2/5

Figure 3

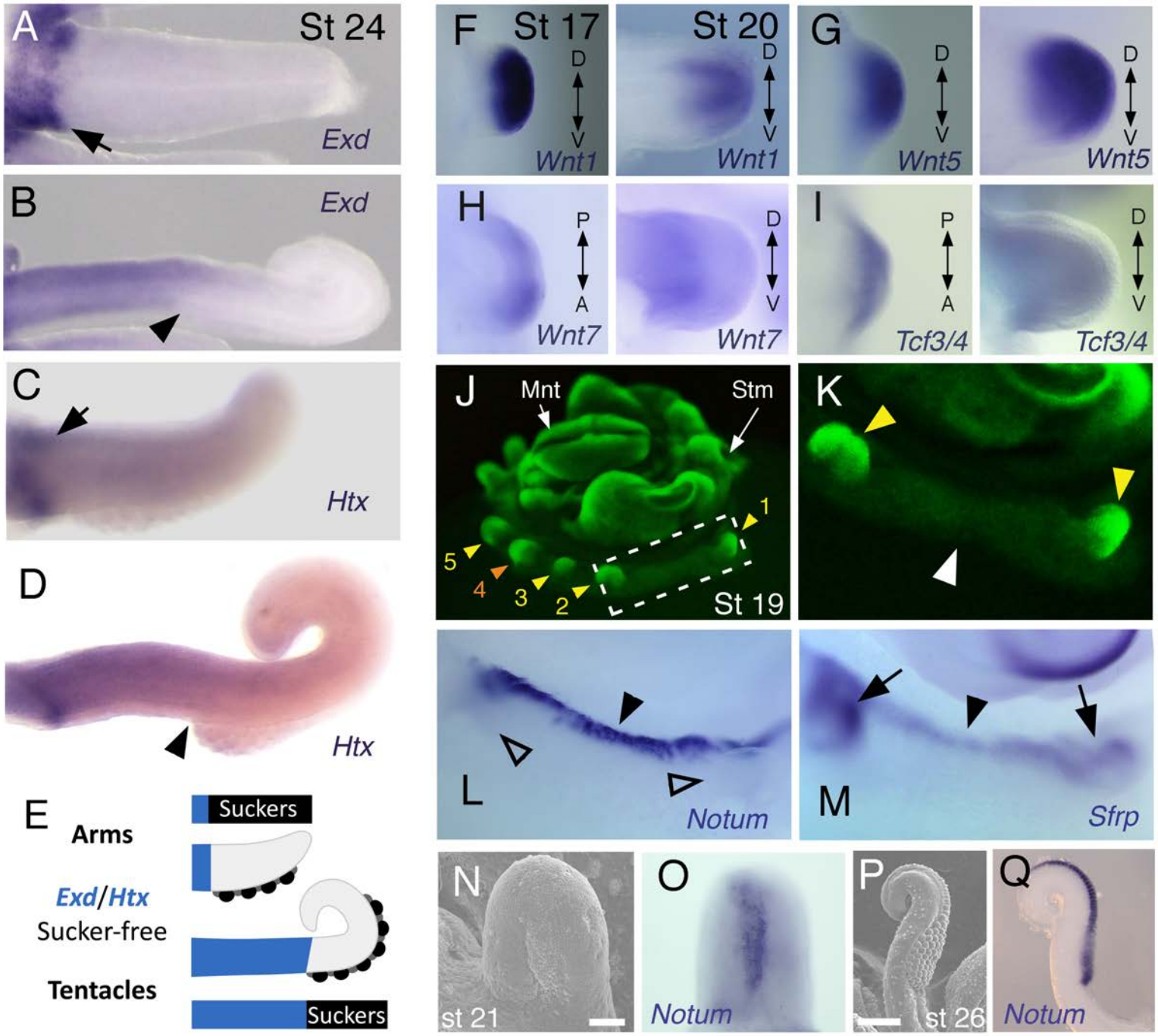
A
St 24
Exd
B
Exd
C
Htx
D
Htx
E
Arms
Suckers
Exd/Htx
Sucker-free
Tentacles
Suckers
F
St 17
D
V
Wnt1
St 20
D
V
Wnt1
G
D
V
Wnt5
D
V
Wnt5
H
P
A
Wnt7
D
V
Wnt7
I
P
A
Tcf3/4
D
V
Tcf3/4
J
Mnt
Stm
1
2
3
4
5
St 19
K
L
Notum
M
Sfrp
N
st 21
O
Notum
P
st 26
Q
Notum

Figure 4

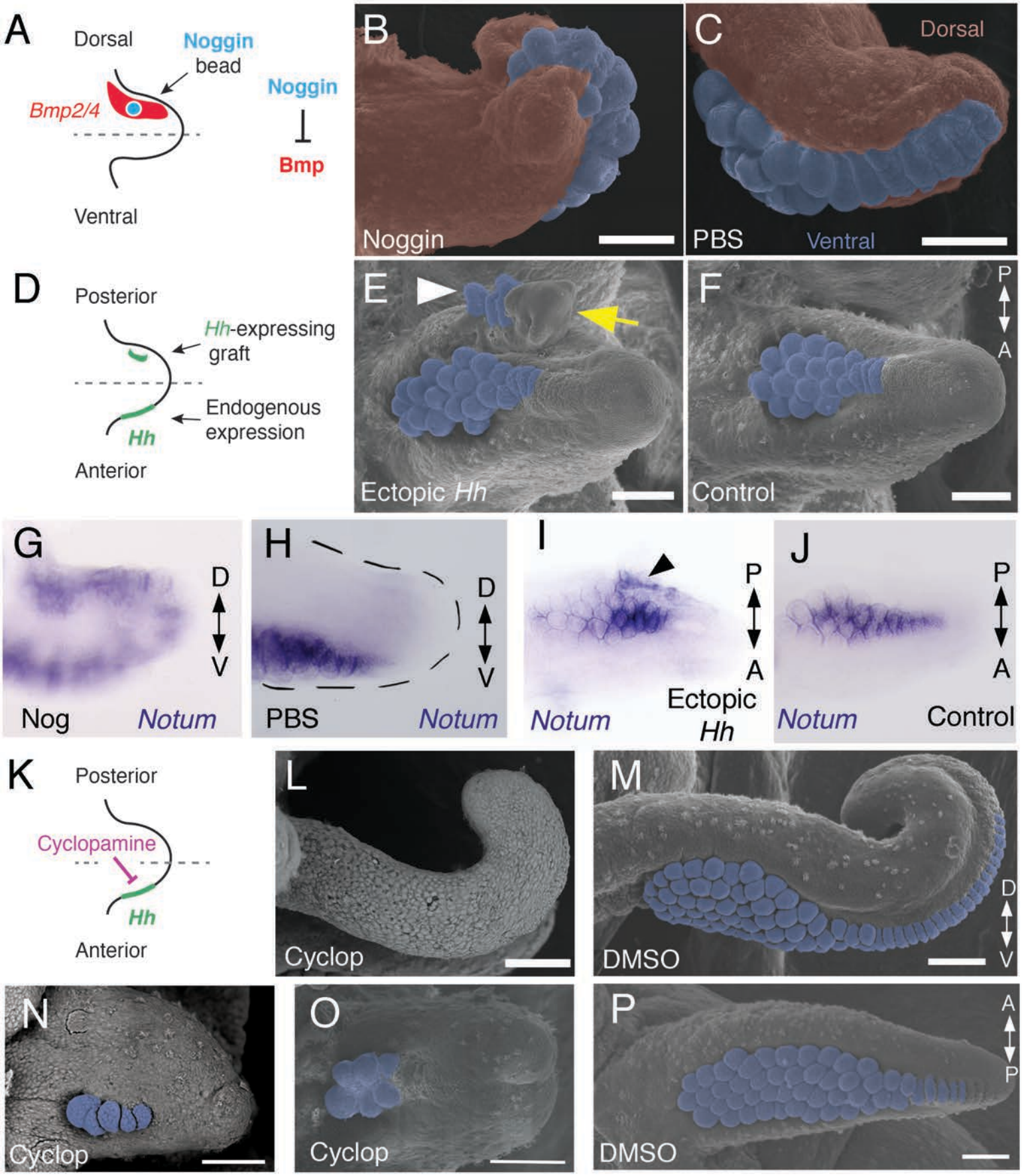
A
Dorsal
Noggin
bead
Bmp2/4
Noggin
Bmp
Ventral
B
Noggin
C
Dorsal
PBS
Ventral
D
Posterior
Hh-expressing
graft
Endogenous
expression
Hh
Anterior
E
Ectopic Hh
F
P
A
Control
G
D
V
Nog
Notum
H
D
V
PBS
Notum
I
P
A
Notum
Ectopic
Hh
J
P
A
Notum
Control
K
Posterior
Cyclopamine
Hh
Anterior
L
Cyclop
M
D
V
DMSO
N
Cyclop
O
Cyclop
P
A
P
DMSO

Figure 1- figure supplement 1

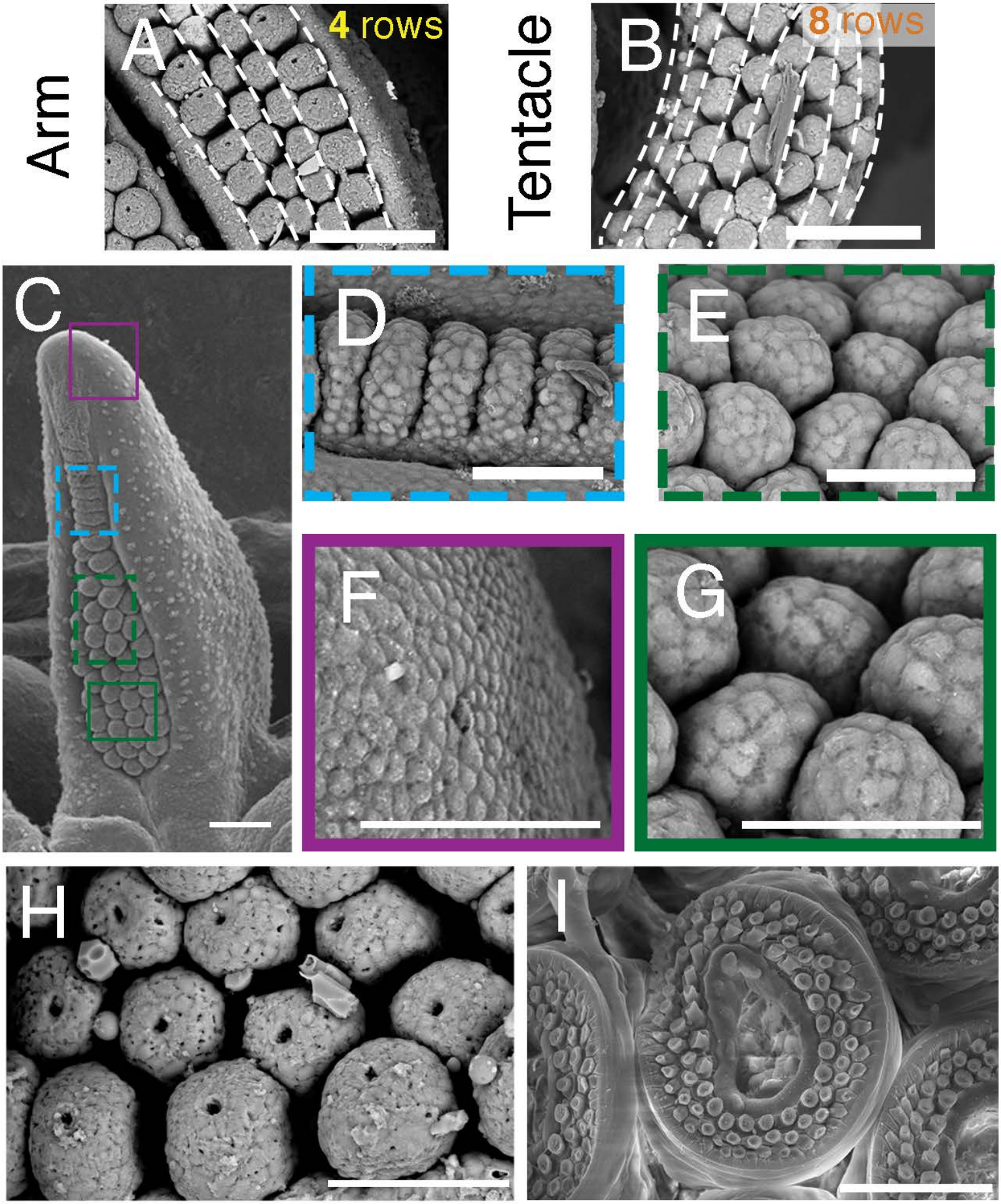

Figure 2- figure supplement 1

Figure 2- figure supplement 2

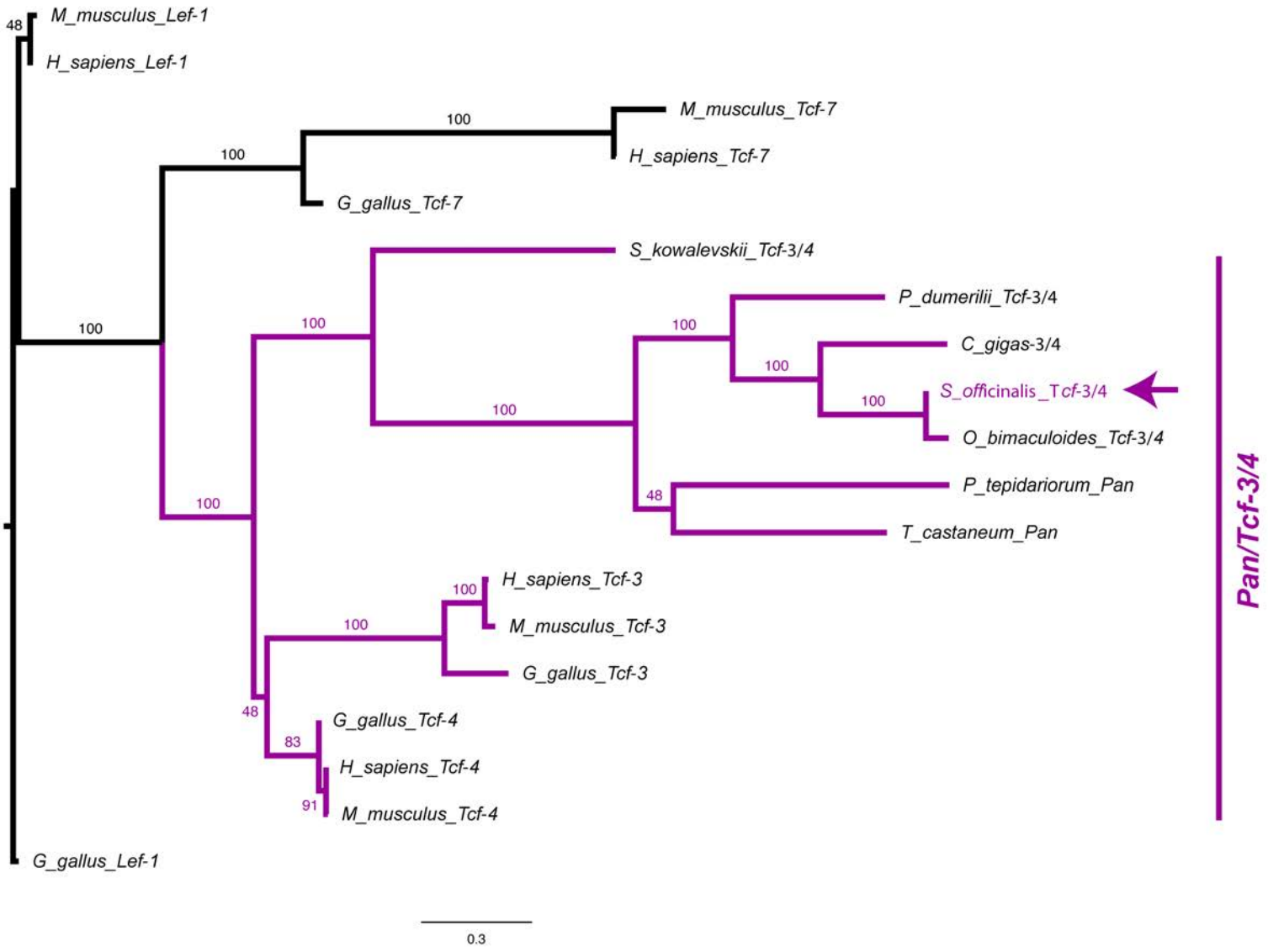

Figure 2- figure supplement 3

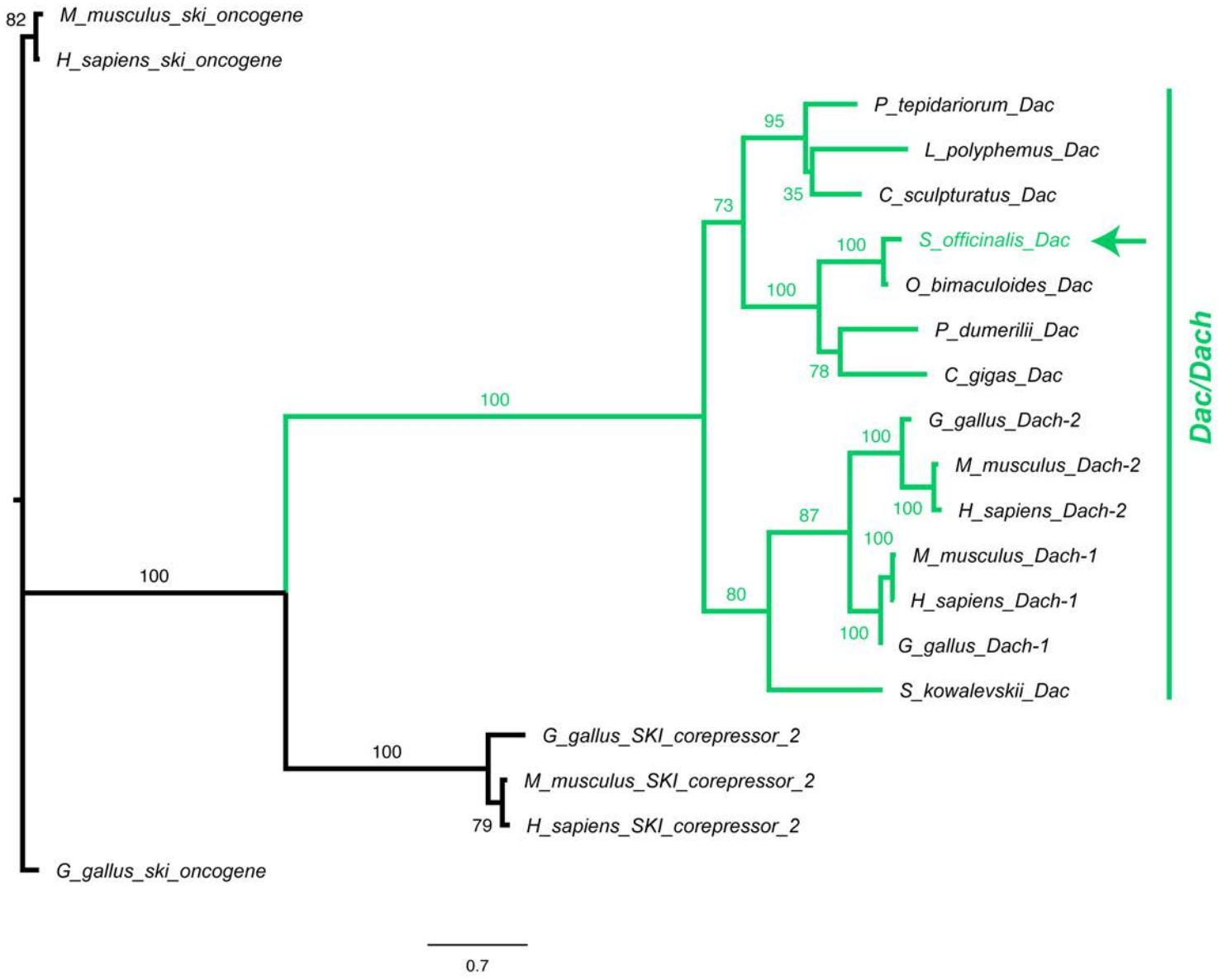

Figure 2- figure supplement 4

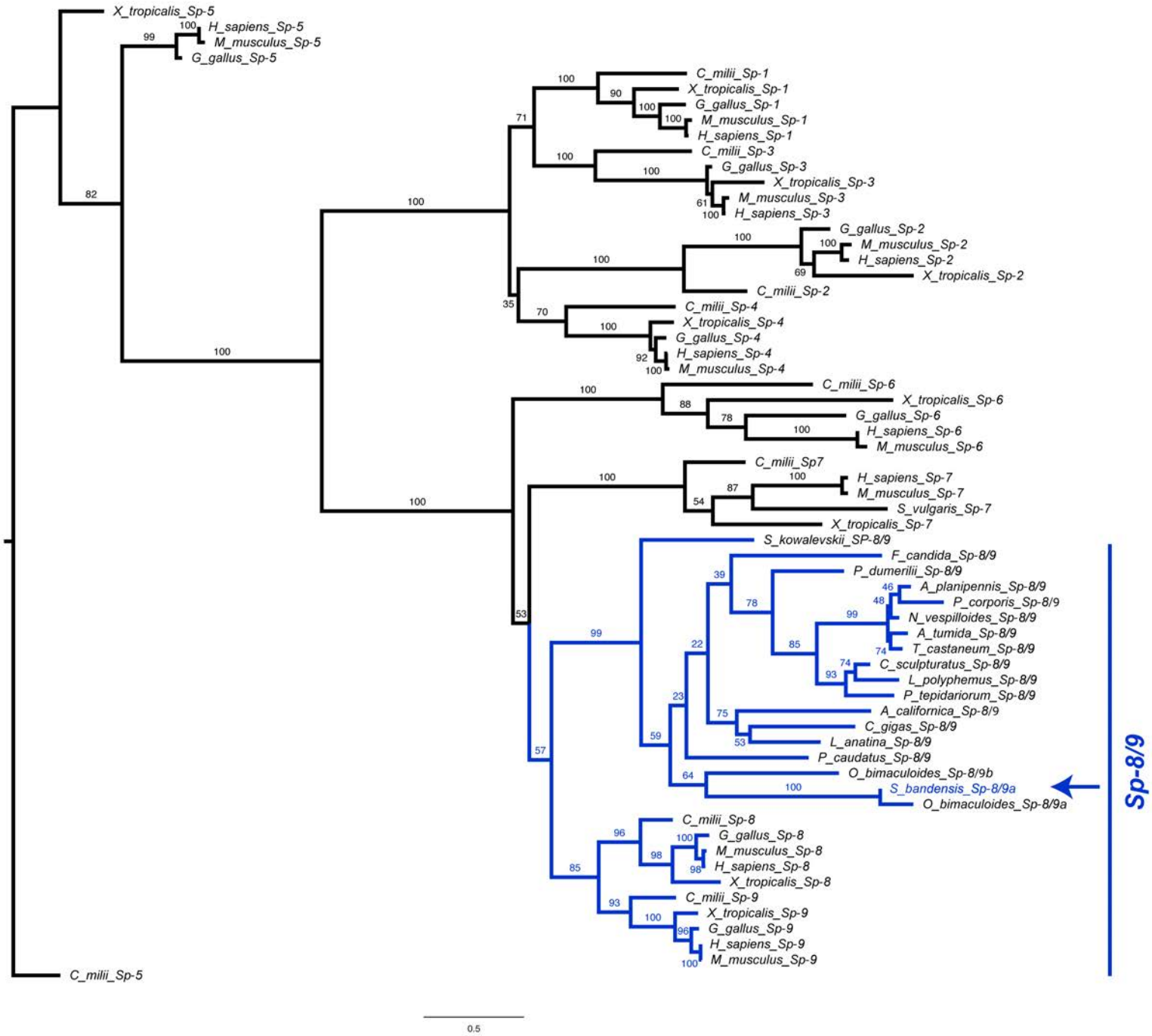

Figure 2- figure supplement 5

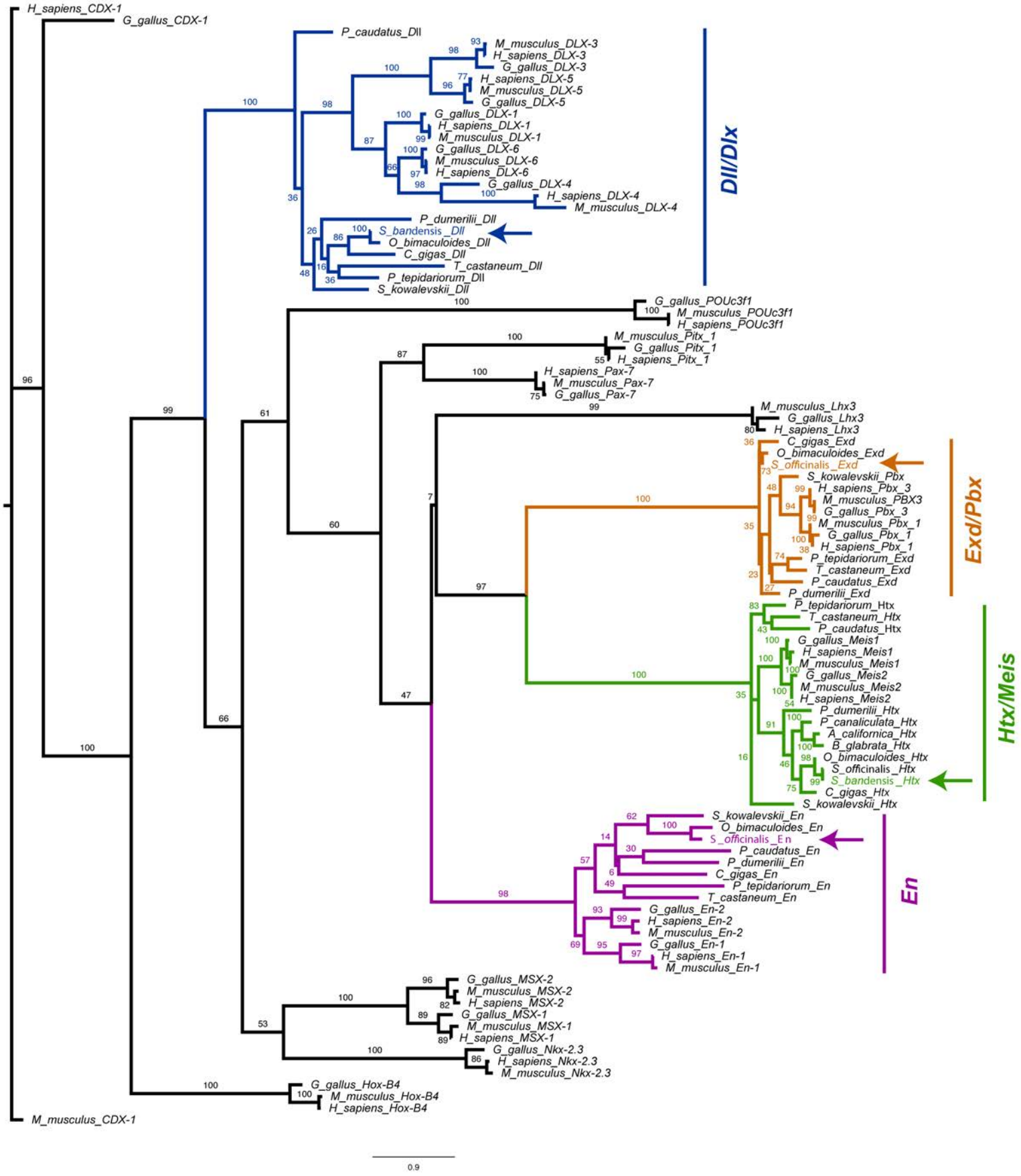

Figure 2- figure supplement 6

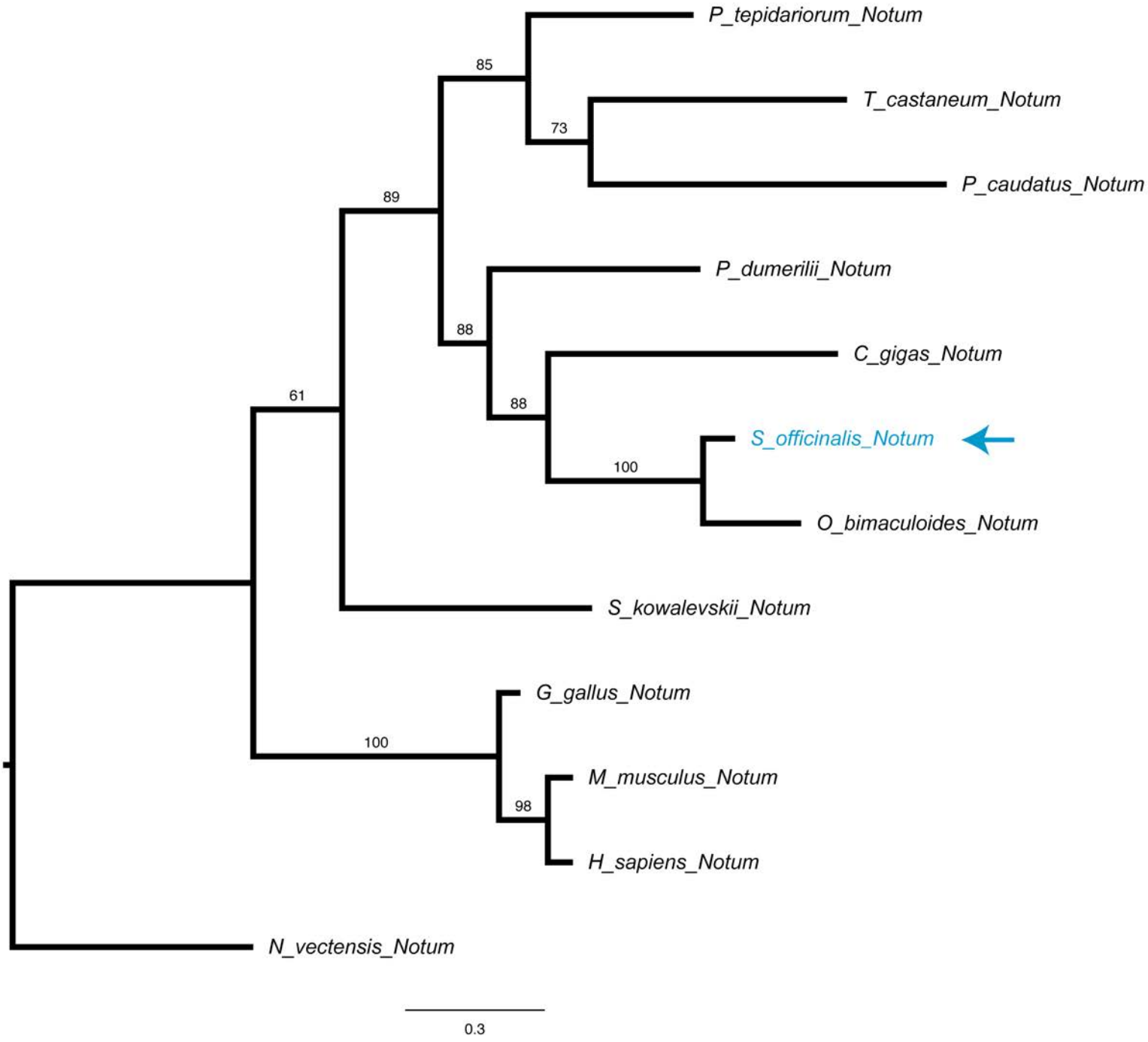

Figure 2- figure supplement 7

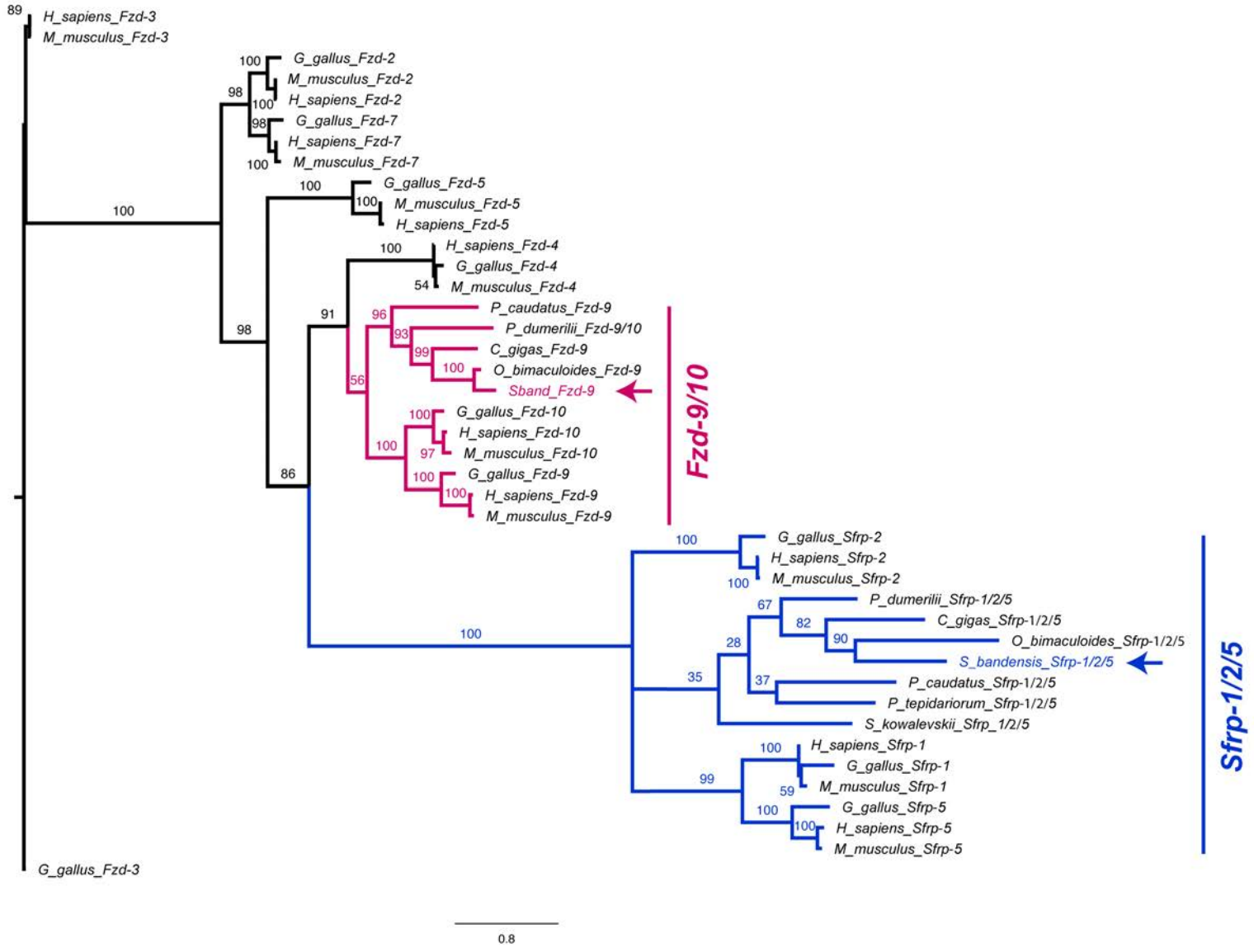

Figure 2- figure supplement 8

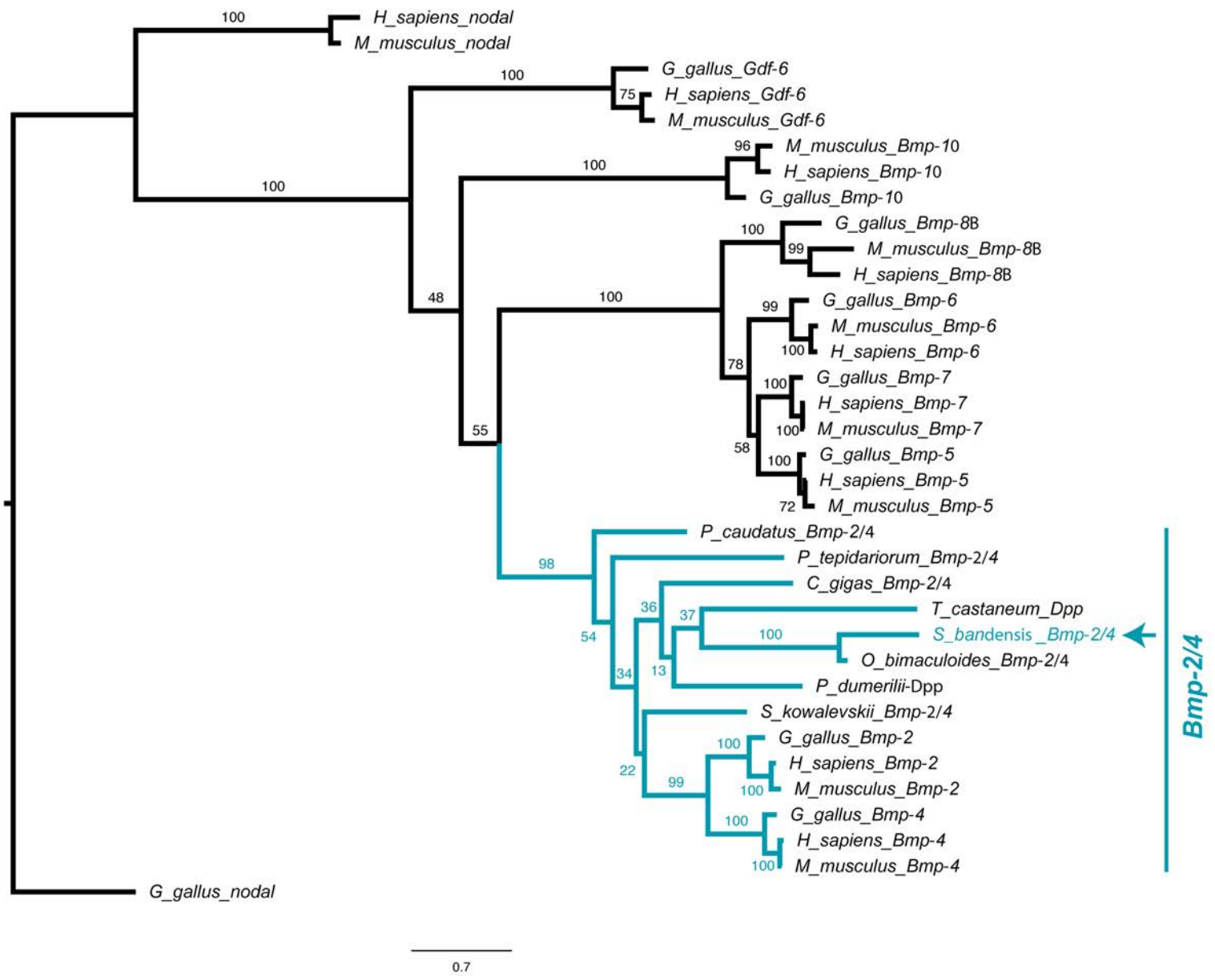

Figure 2- figure supplement 9

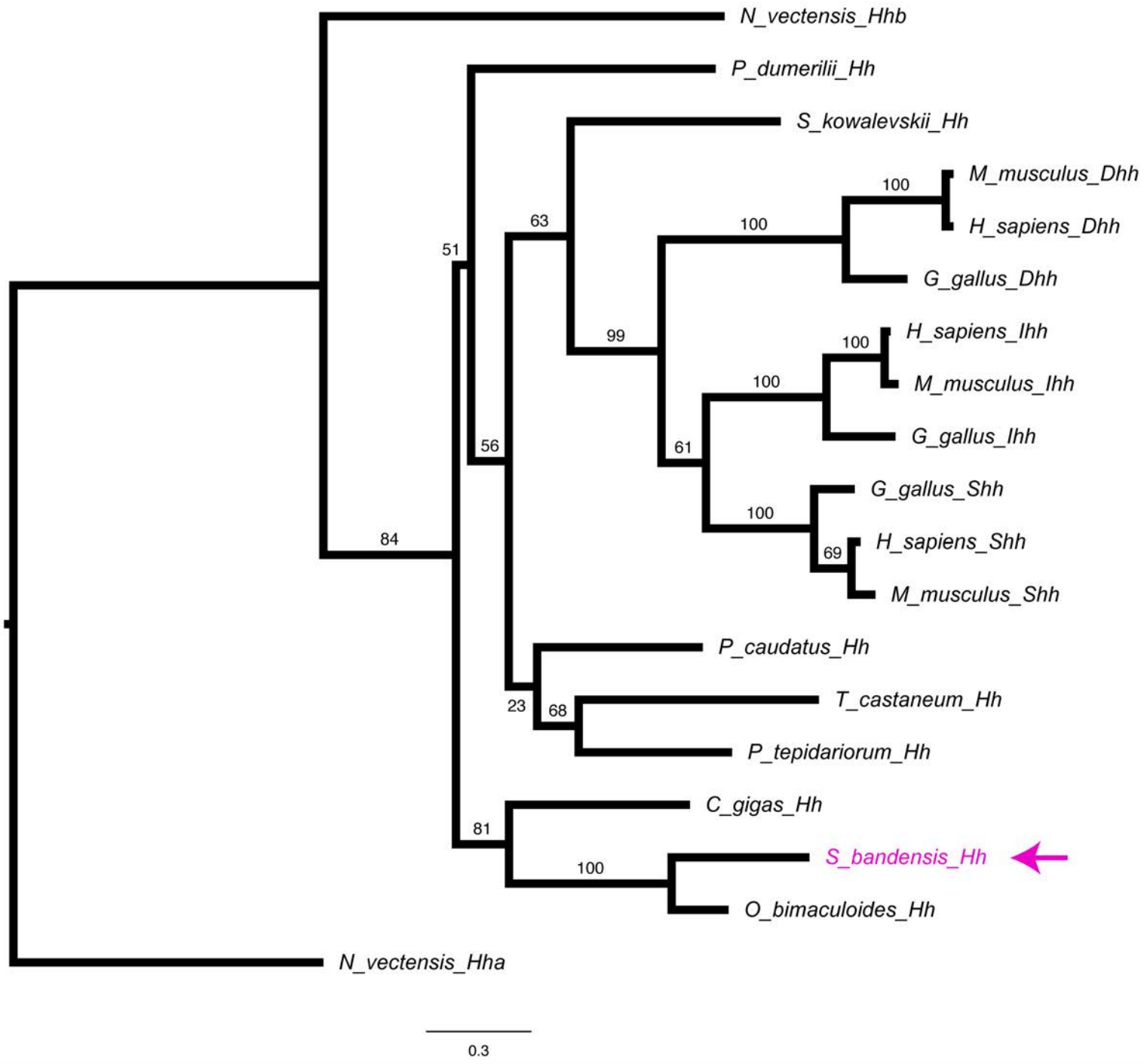

Figure 2- figure supplement 10

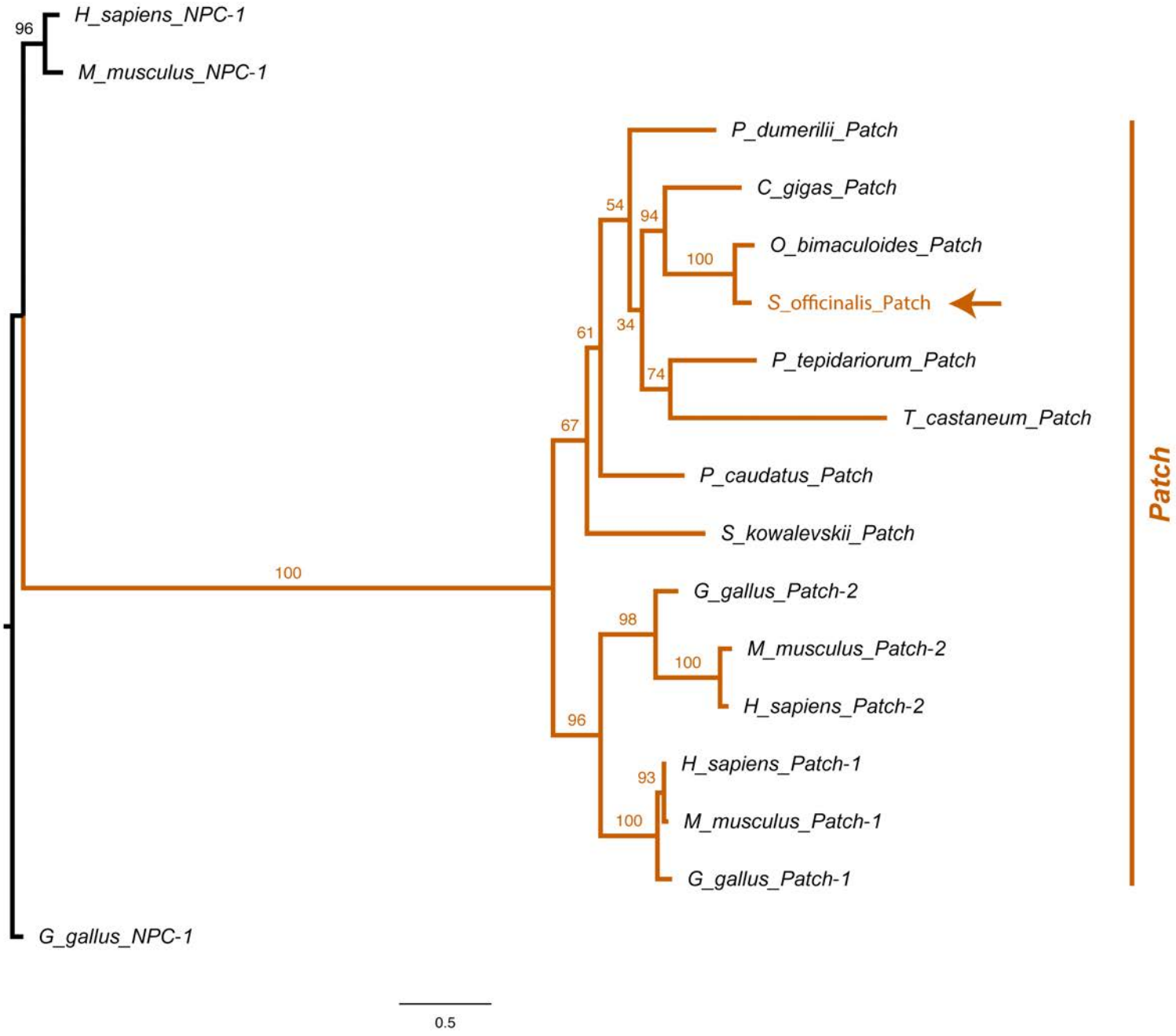

Figure 3- figure supplement 1

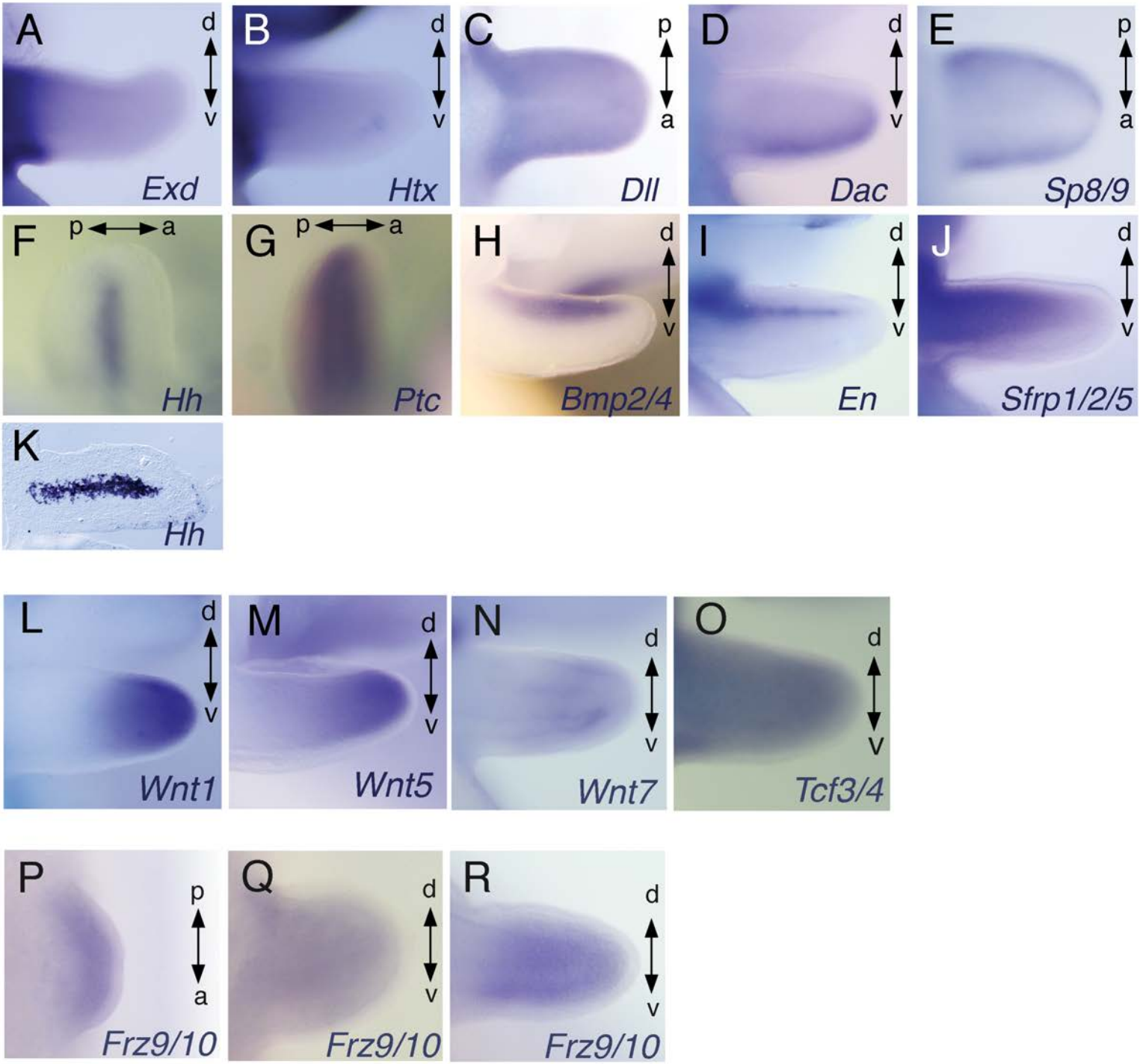

Figure 4 - figure supplement 1

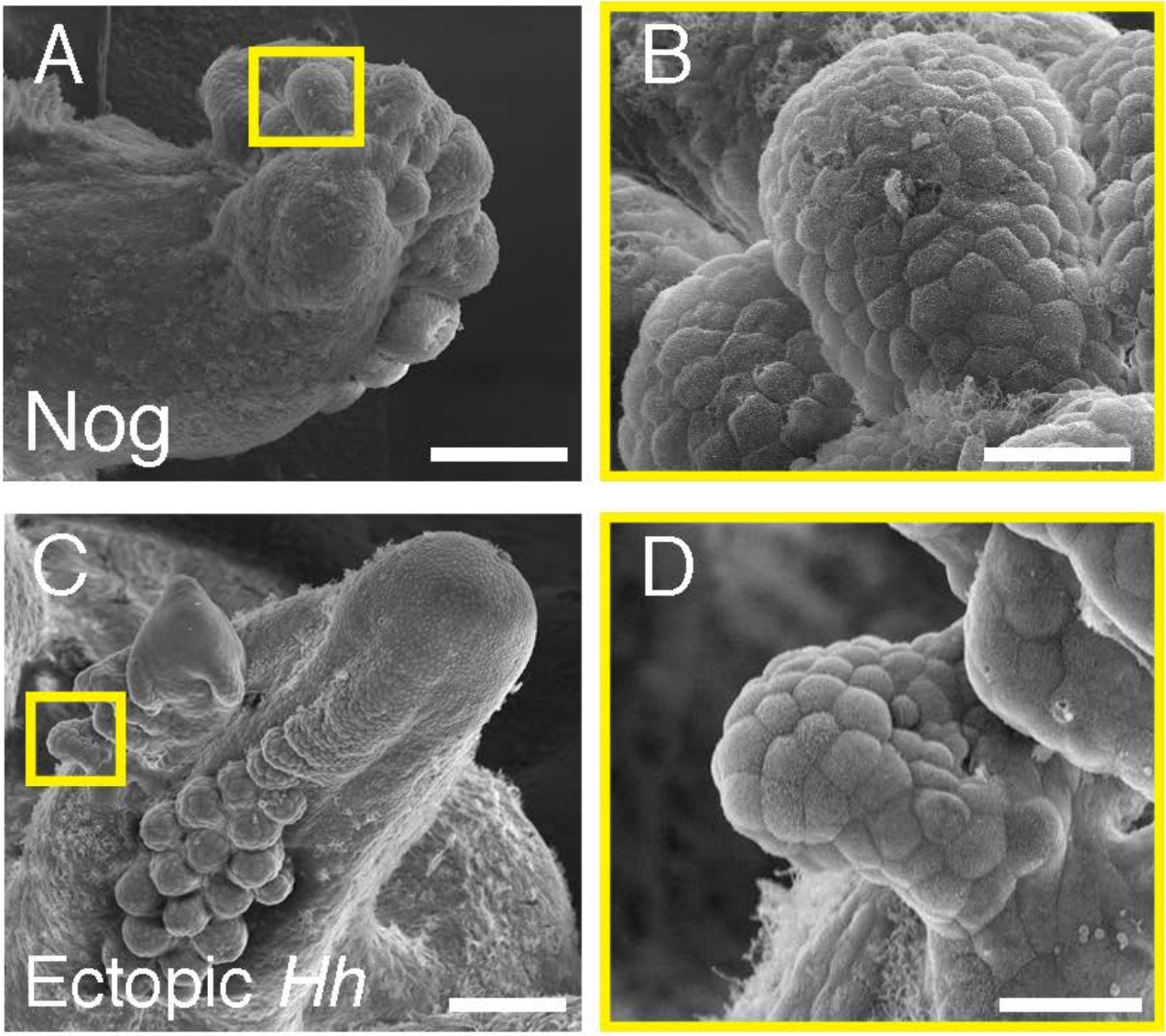
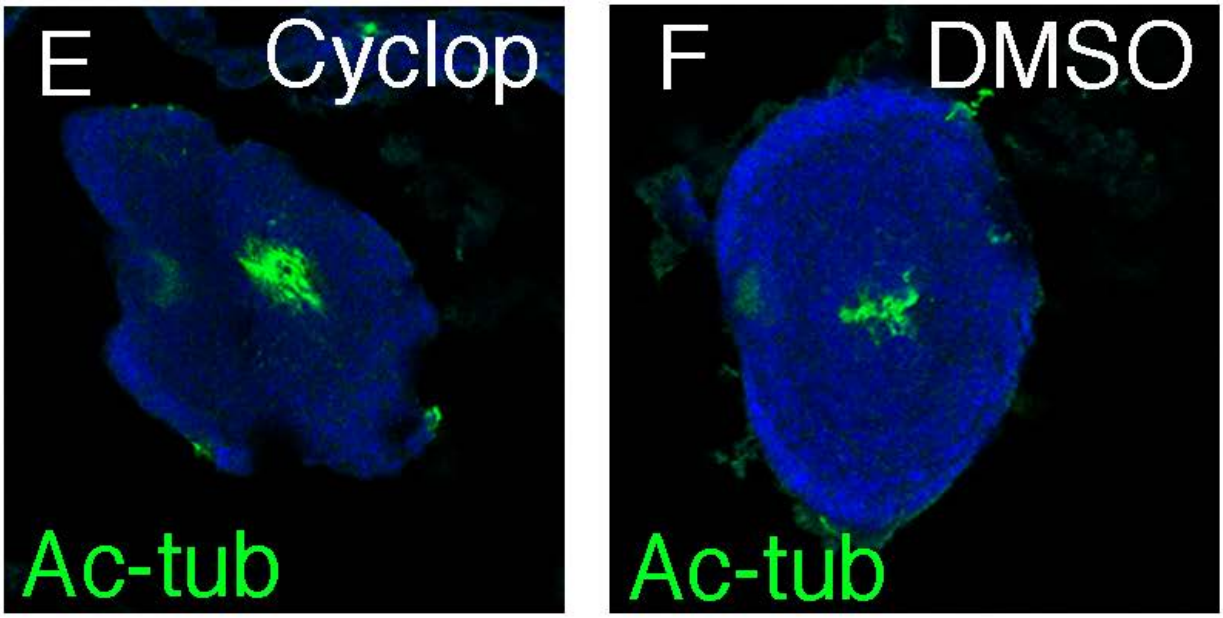
Brachial nerve differentiation